Tutorial 5
Advances in neuroscience methods
2024

Dr. A. Constanti

What interesting advances have there been in neuroscience recording methods over the years?

Advances in neuroscience methods

Over the past years, electrophysiological and other measurement techniques in neuroscience have become more and more advanced, to the point where in some cases, skilled operators and bulky sophisticated equipment are no longer required!

The Nanion Port-a-Patch system. The world's smallest patch clamp setup.

Automated patch clamp recording

- One good example of this is the so-called **automated patch clamp technique**, most suited for cells in suspension culture. The method uses specially constructed microchips with tiny (1-2 μm) holes made in a planar substrate instead of patch pipettes to create the gigaseal mechanically, and then record from single cells.
- It can also be adapted for the automated patch clamping of cultured cells grown on the recording chip or slices of brain tissue. The patch chip systems are quite expensive but have the added benefit of hands-free operation and no requirement for elaborate patch-rig assemblies.

Automated patch clamp recording

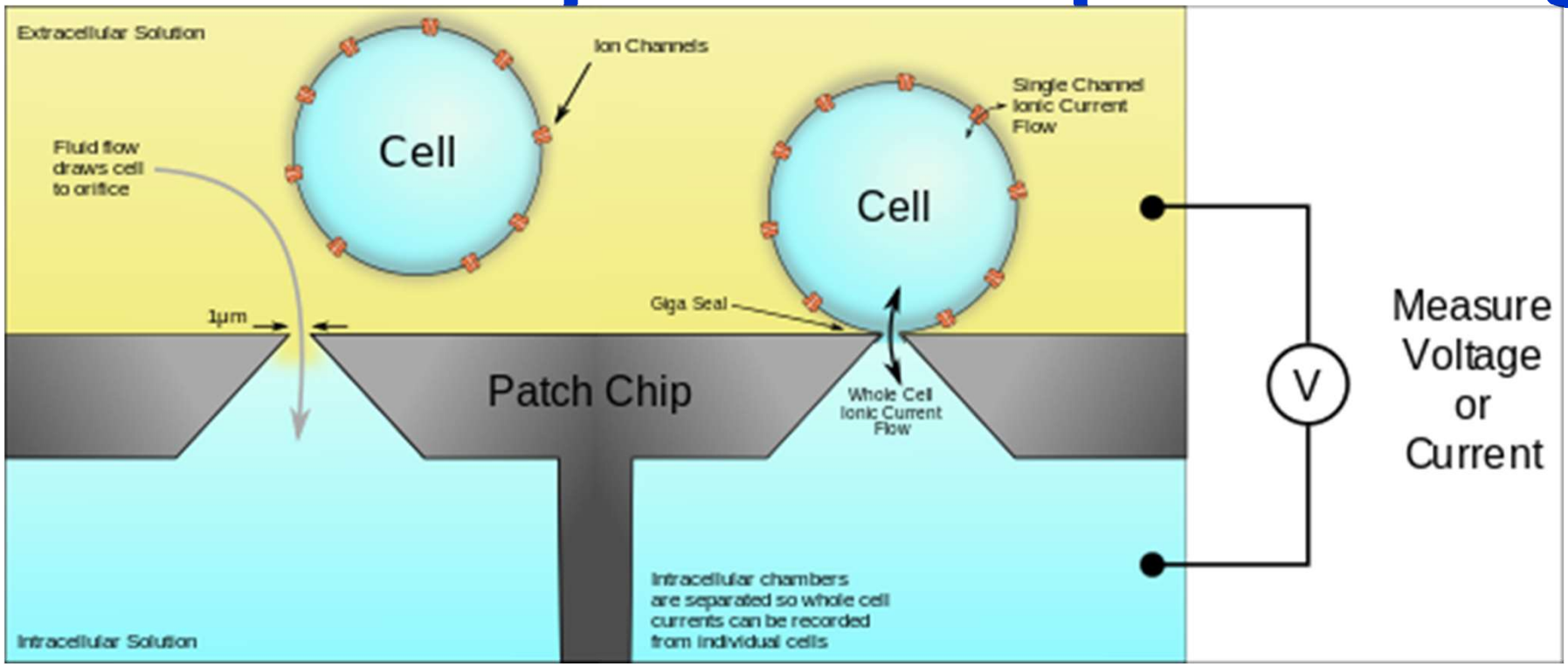

A schematic of a patch clamp chip showing how a gigaseal is first formed on a single cell in suspension, then with automated suction, the whole cell recording configuration is achieved allowing whole cell currents to be recorded. Automated patch clamp increases throughput and ease of use compared to the conventional patch clamp technique making it accessible to a wider audience.

Automated patch clamp recording

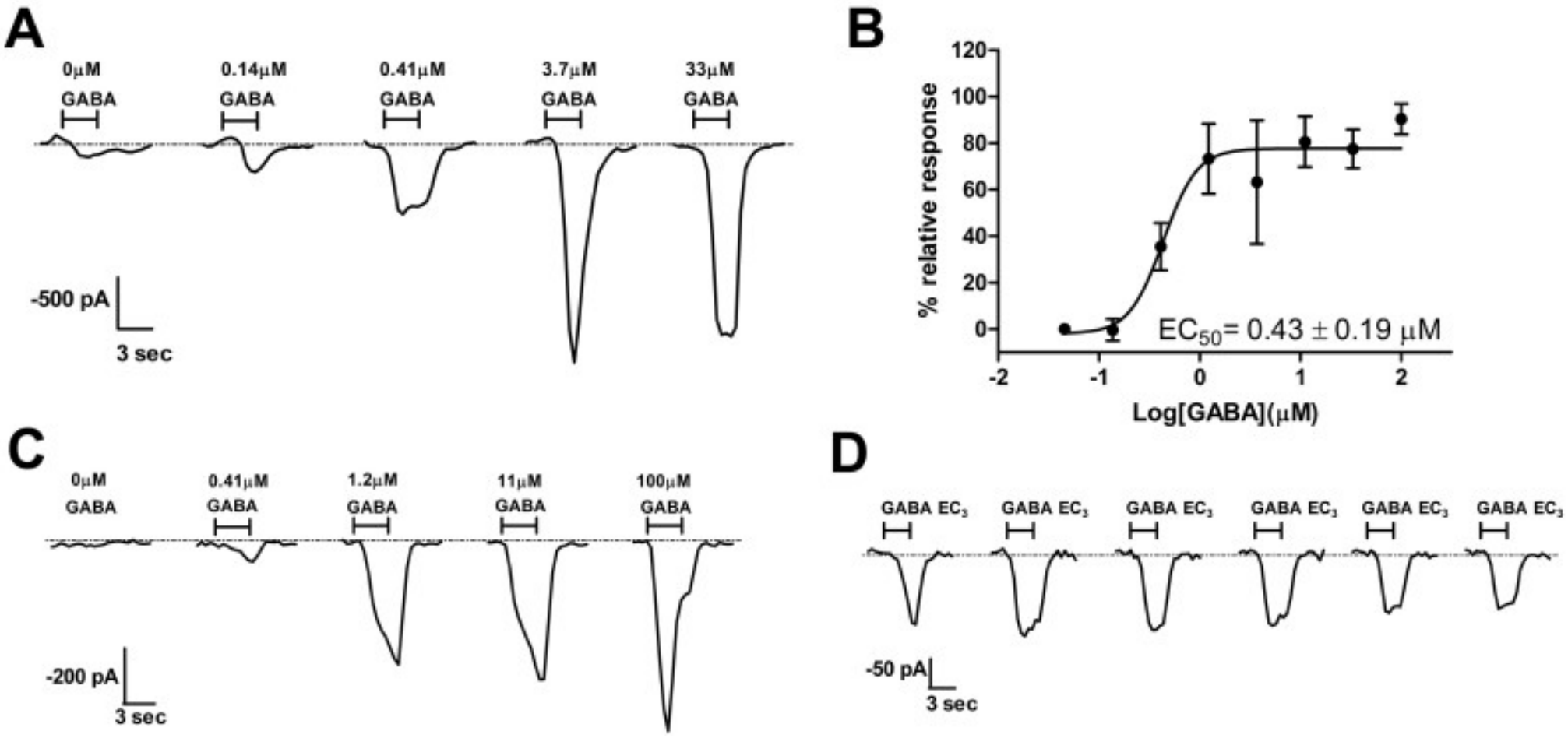

Characterization of **GABA currents** measured with an automated patch-clamp using **human neurones derived from pluripotent stem cells (iCells).**

Yuan et al., (2016). J Pharmacol Toxicol Methods;82:109-114.

Automated patch clamp recording

Automated patch clamp is now used routinely by large drug companies for high-throughput screening (HTS) and safety testing of new drugs for specific target ion channels or receptors. The latest high-throughput patch-clamp instruments such as the **SyncroPatch 384PE** can record from **384** or **768** wells simultaneously, giving an unprecedented throughput for patch-clamp experiments. Storage and analysis of data have also vastly improved enabling large amounts of data to be recorded and analyzed in a comparatively short space of time.

For a recent review see: Obergrussberger *et al*., (2020) Automated patch clamp in drug discovery: major breakthroughs and innovation in the last decade. Expert Opin Drug Discov Jul 10;1-5. doi: 10.1080/17460441.2020.1791079

Automated patch clamp recording

The **SyncroPatch 384/768** automated patch clamp engine is a novel system allowing records of up to **738** cells simultaneously using a pipetting robot system. All cells are recorded in parallel allowing throughput of up to 20K data points per day.

Automated patch clamp recording

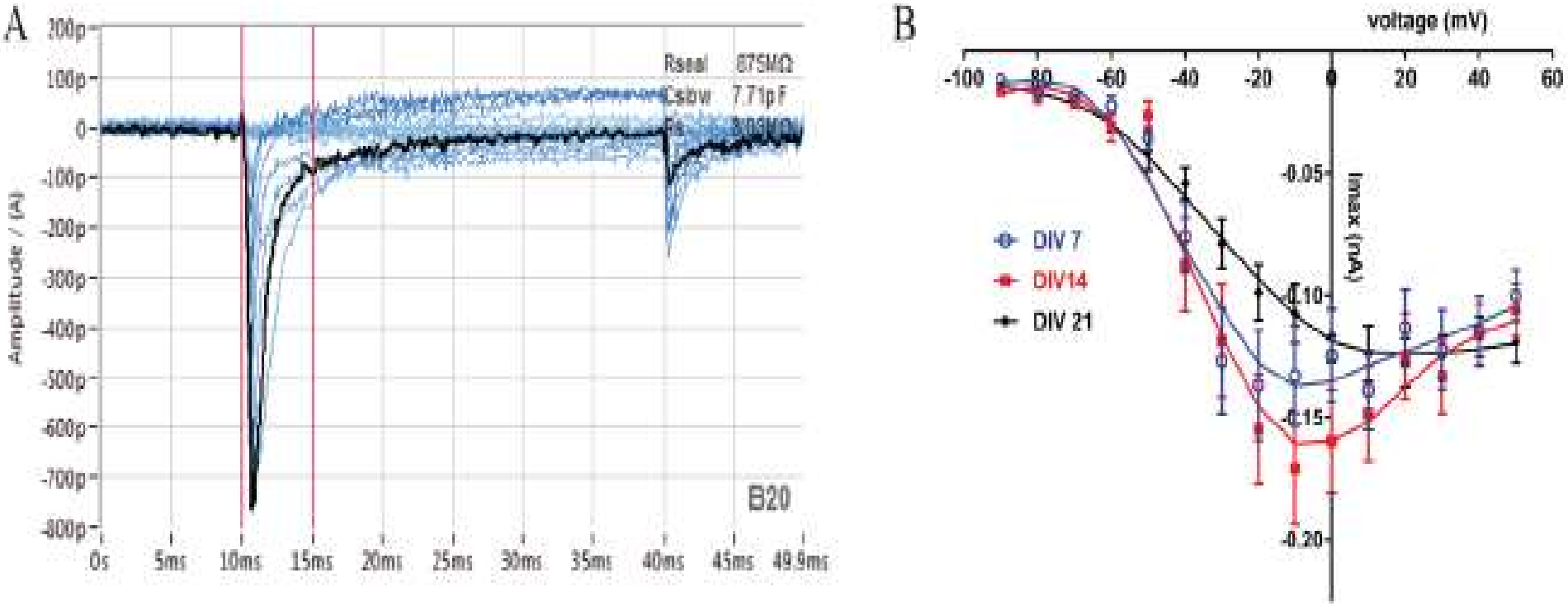

(A). I-V relationship of Na^+ currents recorded from a **cultured rat cortical neurone (DIV 14)** on the **SyncroPatch 384PE**. Currents were evoked using voltage steps from –90 to +50 mV with 10 mV increments. (B) Population I-V curves for the peak inward Na^+ currents plotted for all DIVs with internal Cs^+ to block outward K^+ conductances.

Toh *et al* (2020) SLAS Discovery 25(5) 447–457

Automated patch clamp recording

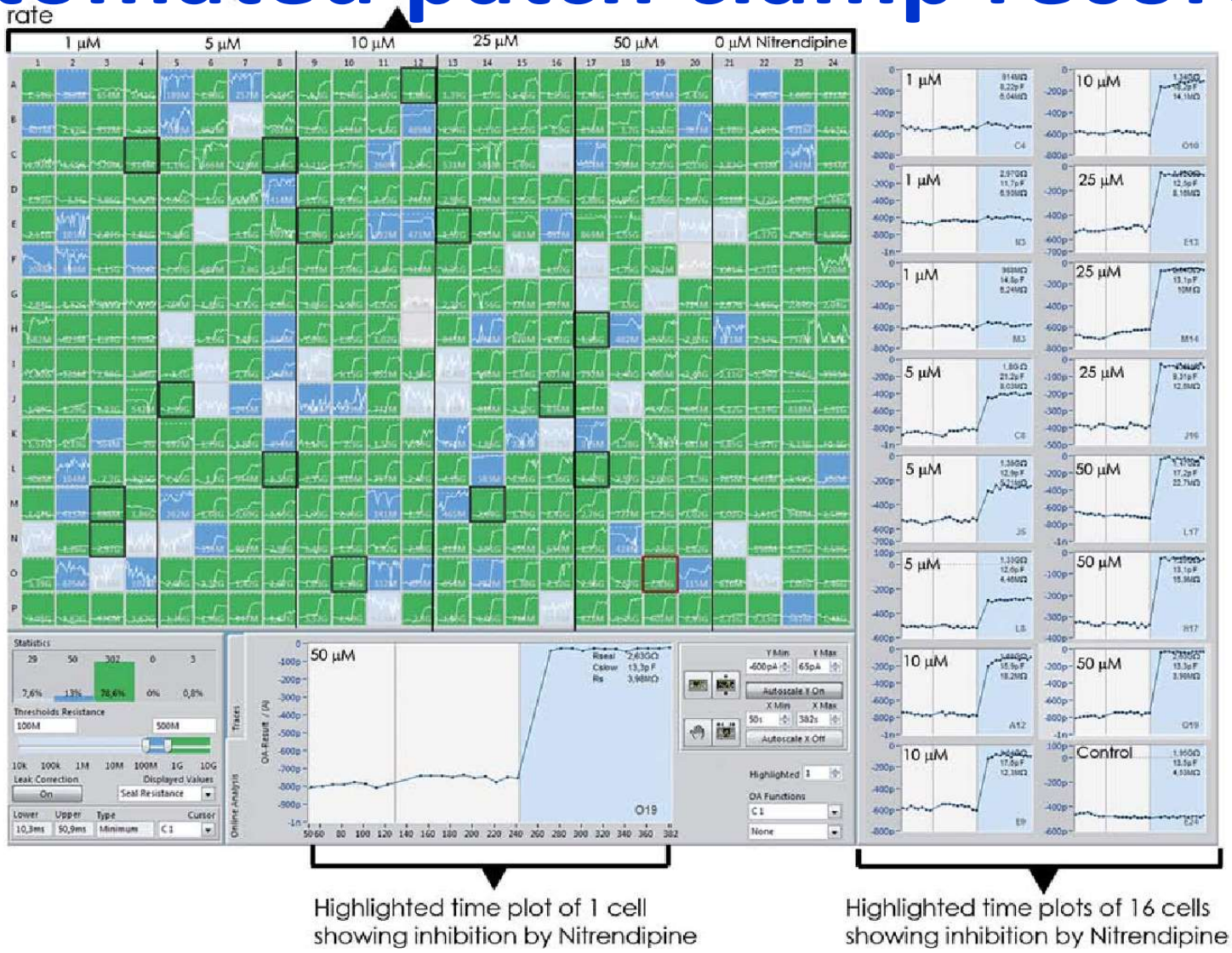

Graphical display used on the **SyncroPatch 384PE**. Screenshot of depiction of online analysis data of **$Ca_V3.2$ (T channel)-expressing HEK cells** as recorded on one NPC-384 patch clamp chip.

Is it possible to do automated *in vivo* patch clamp recordings?

In vivo automated patch clamp recording

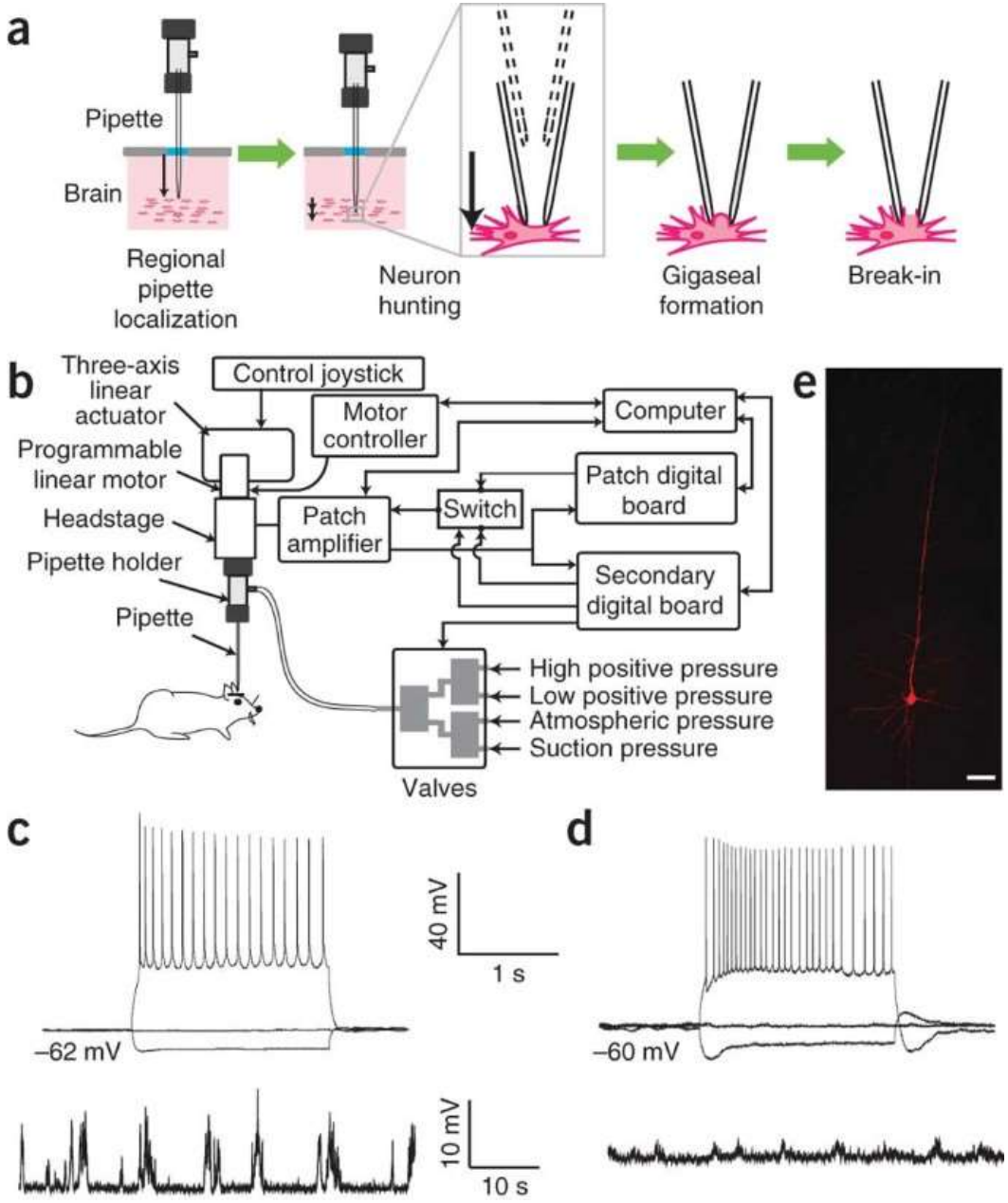

Remarkably, in the last decade, it has also been possible to develop a robot system that automatically performs patch clamping *in vivo*, detecting cells by analyzing the temporal sequence of electrode impedance changes as it is step advanced through the brain tissue. A good yield, and quality of automated whole cell recordings have been obtained in **mouse cortex and hippocampus**.

Kodandaramaiah et al., (2012) Nature Methods 9, 585–587.

In vivo automated patch clamp recording

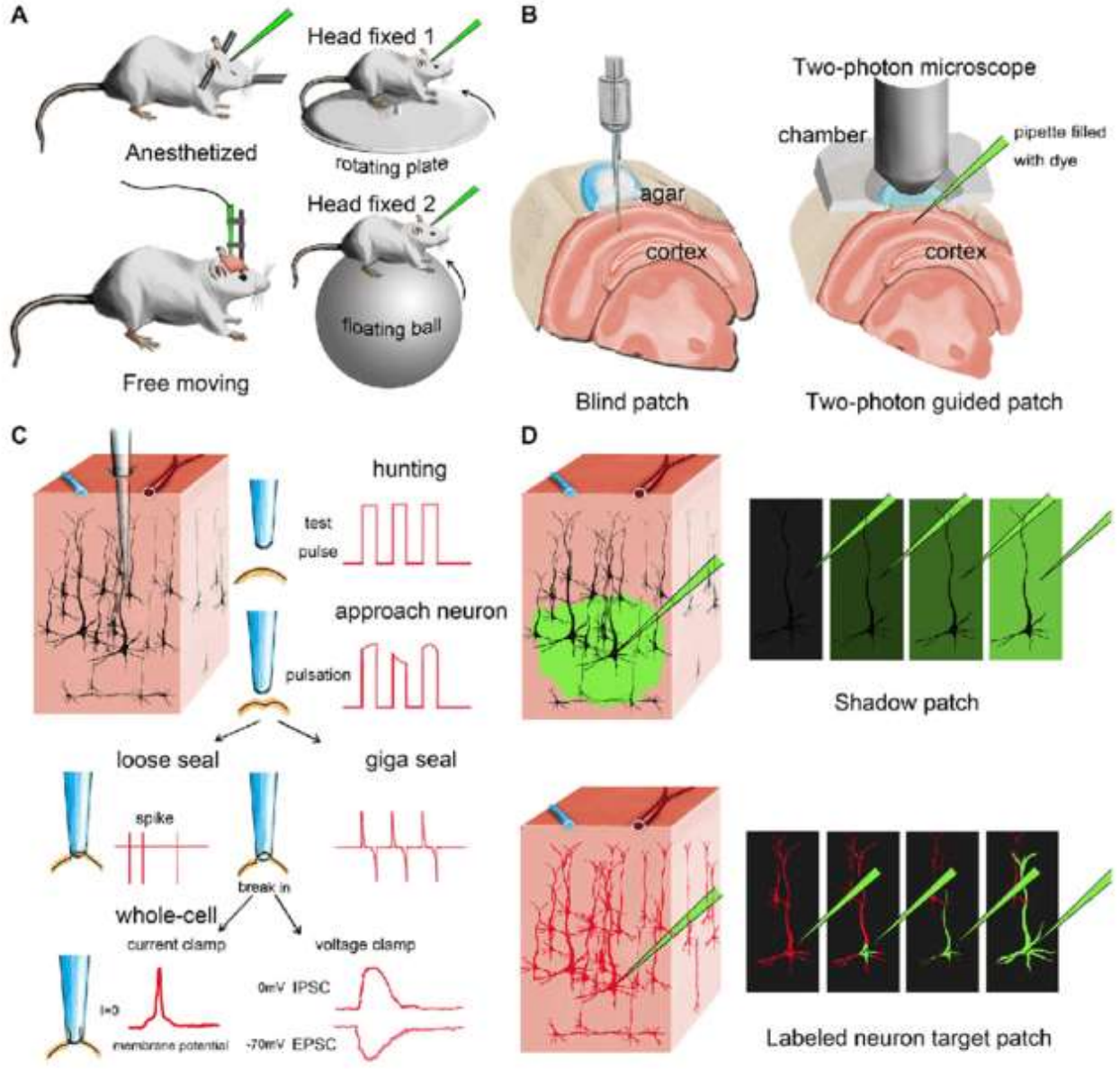

Two-photon guided patch clamp can target specific neurones using fluorescence guidance.

Tao et al (2015) Frontiers in Neural Circuits, 9 Article 23

What other advances have there been in multi-site recording?

Multielectrode arrays (MEAs)

- **MEAs** were originally developed with the specific aim of allowing experimenters to stimulate and record extracellularly from neuronal cultured networks or thin brain slices at multiple positions simultaneously, thus providing a real-time view of the spread of electrical activity across the tissue.

- Early arrays consisted of **8x8** or **16x16** electrodes on a glass substrate, viewed using an inverted microscope, through the bottom of the MEA assembly. The chip was connected to amplifiers and a computer that allowed continuous stimulation or recording from neurones lying on or near electrodes.

Multielectrode arrays (MEAs)

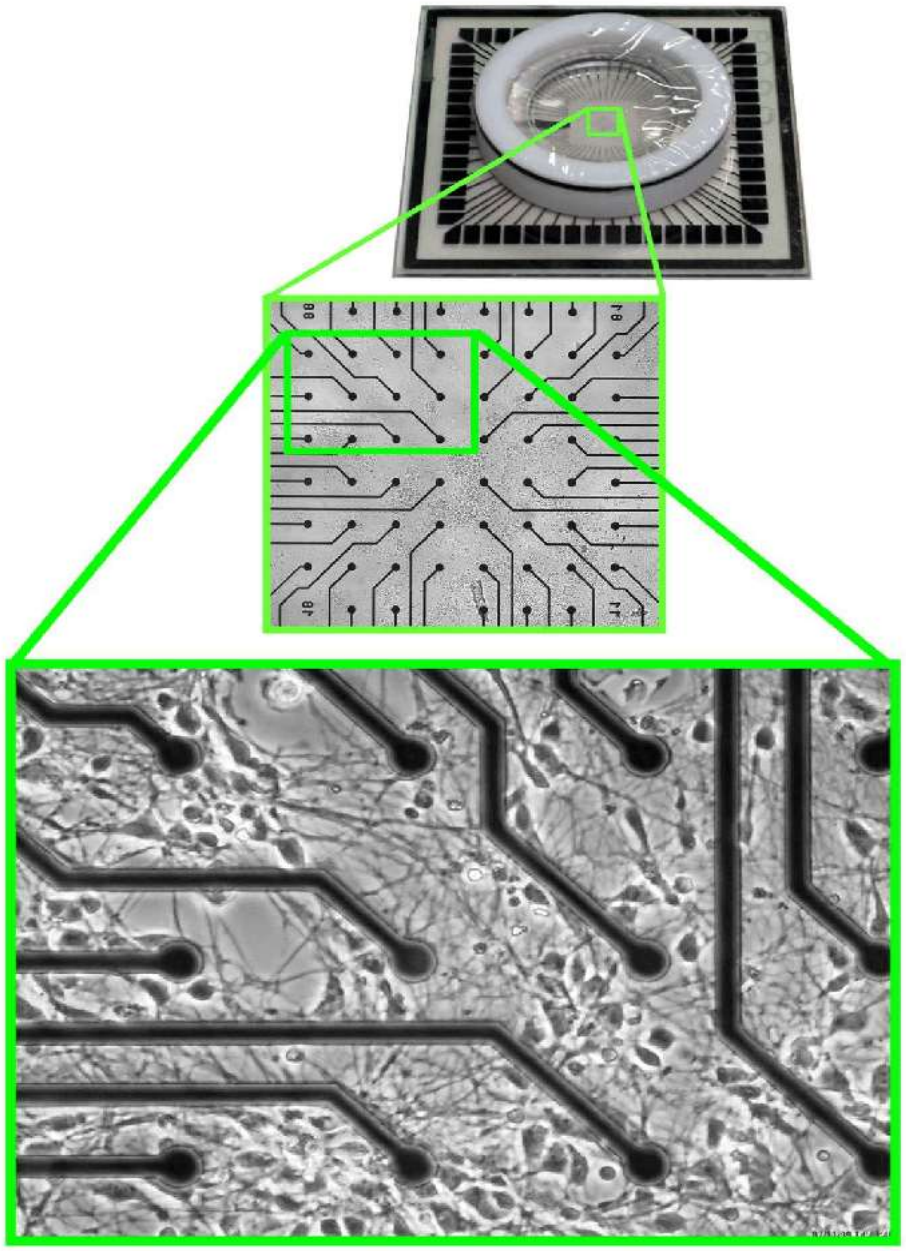

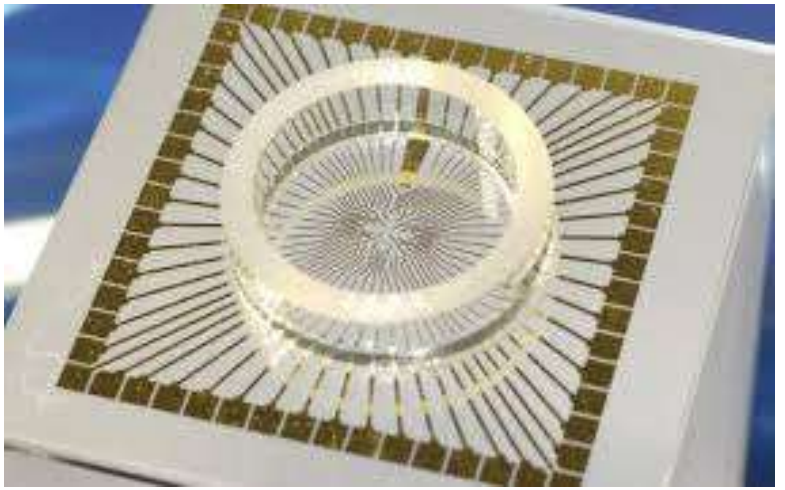

Dissociated cortical culture grown on a multi-electrode array (MEA): An MEA chamber (Top), with an 8 x 8 grid of electrodes (Middle), and neurones growing on the chip at high magnification (Bottom).

Multielectrode arrays (MEAs)

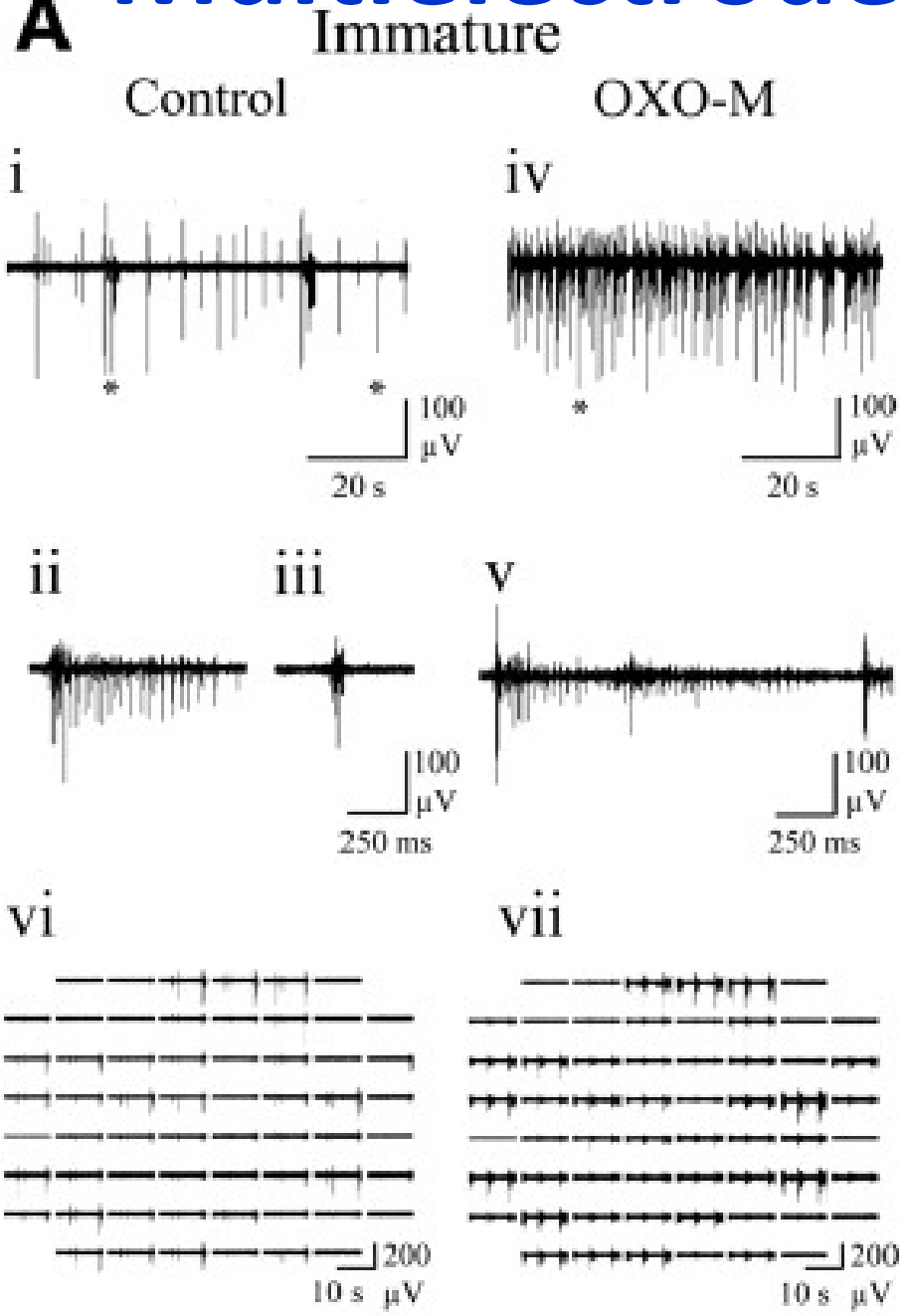

Spontaneous neuronal activity exhibited by an **immature cortical culture** recorded via MEA in control and following application of the **mAChR agonist, OXO-M** (10 µM). (i) 100 s of spontaneous neuronal activity occurring on a single channel. (iv) activity in OXO-M (vi) Array-wide neuronal activity in control conditions and (vii) following addition of OXO-M.

Hammond et al. (2013) BMC Neuroscience 2013, 14:38

Multielectrode arrays (MEAs)

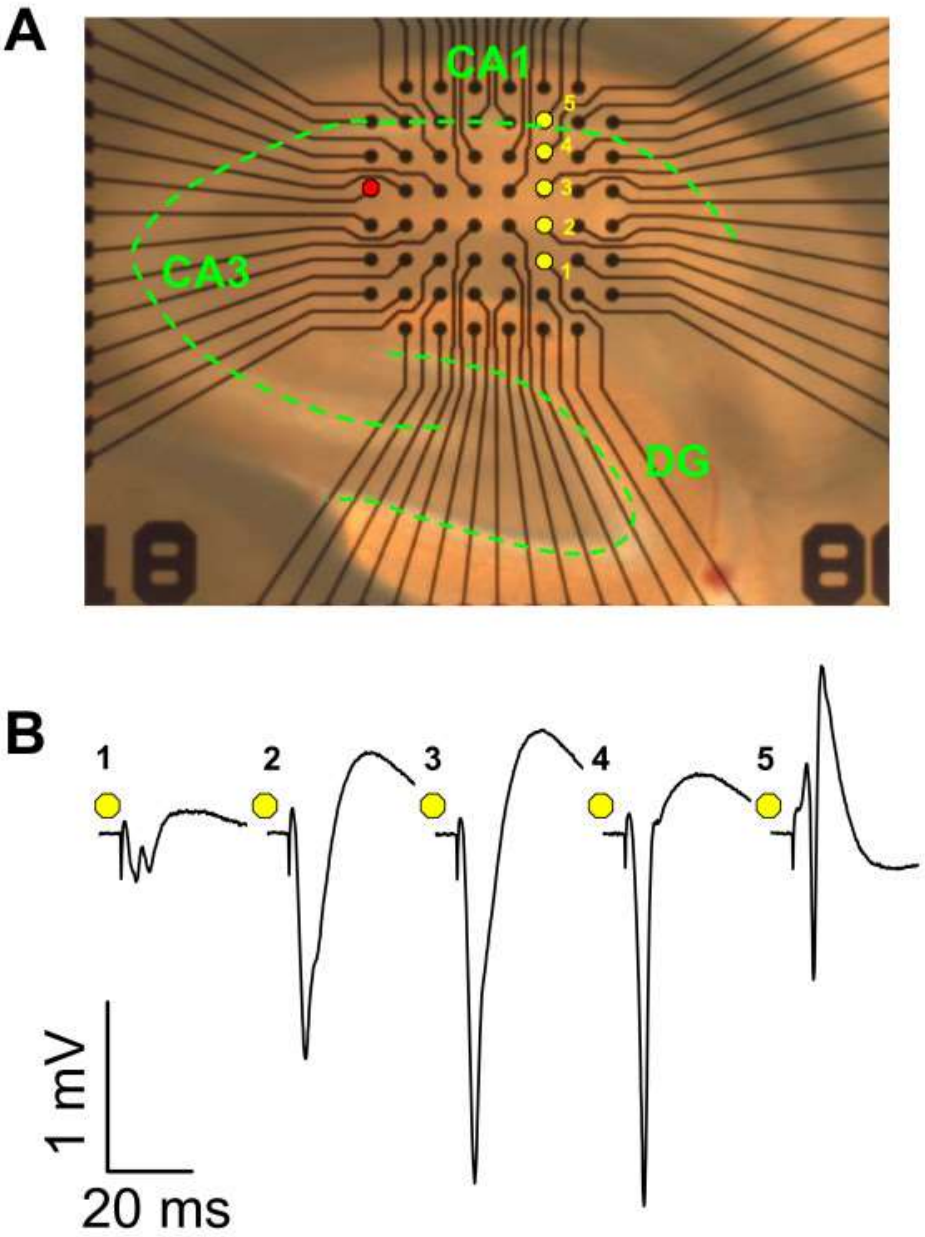

Extracellular fEPSPs recorded in **hippocampal CA1 area** by an MEA A) 350 µm hippocampal slice was placed over 8×8 3D MEA and one electrode (red) was selected for stimulation of Schäffer collateral/commissural fibres. A column of electrodes (yellow) was chosen to record synaptic responses in stratum lacunosum-moleculare (1), stratum radiatum (2–4) and stratum pyramidale/stratum oriens (5). Electrode separation =100 µm. B) fEPSPs recorded by electrodes 1–5.

Multielectrode arrays (MEAs)

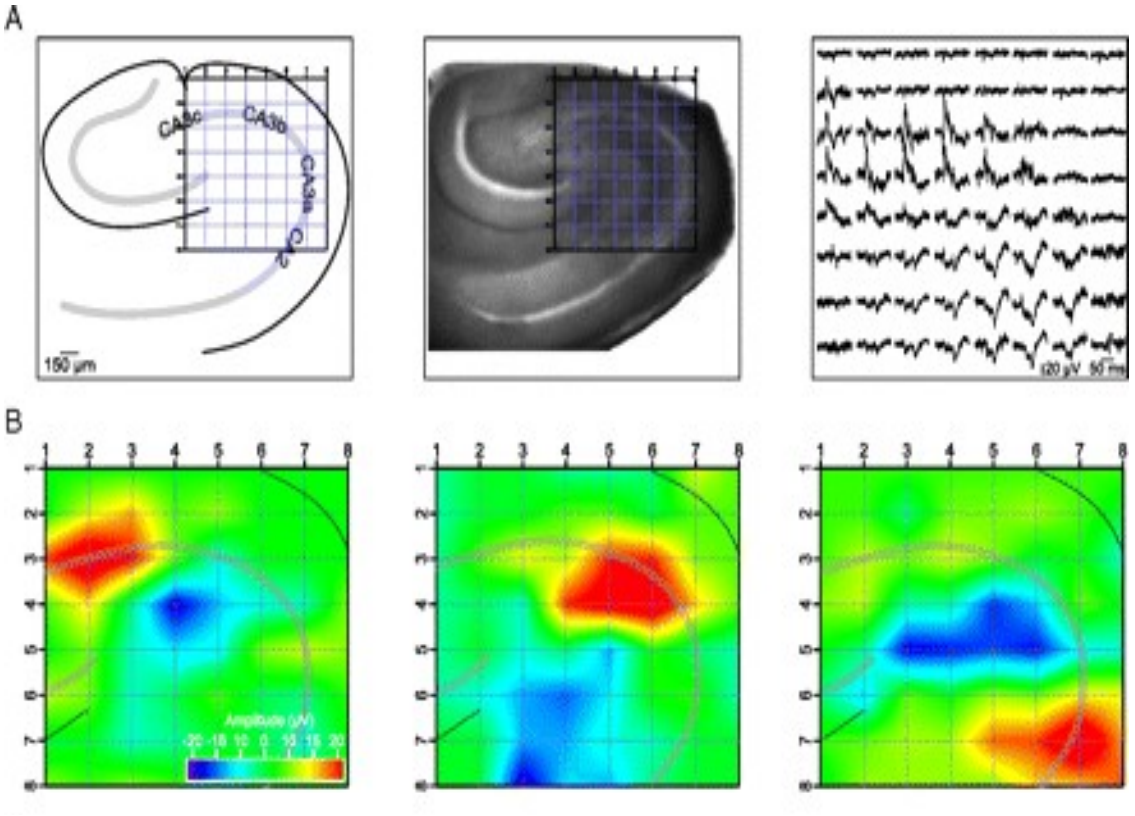

Spontaneous population burst activity (sharp waves) arise locally and independently in all CA3 subfields, similar to those seen during slow-wave sleep *in vivo.* A, **Hippocampal slice on an 8×8 MEA;** Multi-site recording wave shows that the event is localized (right). B, Pseudocolour representation of the voltage deflections observed during three separate sharp waves in the same slice.

Ellender et al (2010). J. Neuroscience, 30 (17) 5979-5991;

Multielectrode arrays (MEAs)

The newest generation high-density **3 Brain microelectrode array (HD-MEA), now features 4,096 low-noise microelectrodes (64x64)** that allow for simultaneous electrophysiological recording at much higher and faster temporal resolution.

https://www.youtube.com/embed/4UVYIyOpeYc

Can MEAs record intracellularly?

Multielectrode arrays (MEAs)

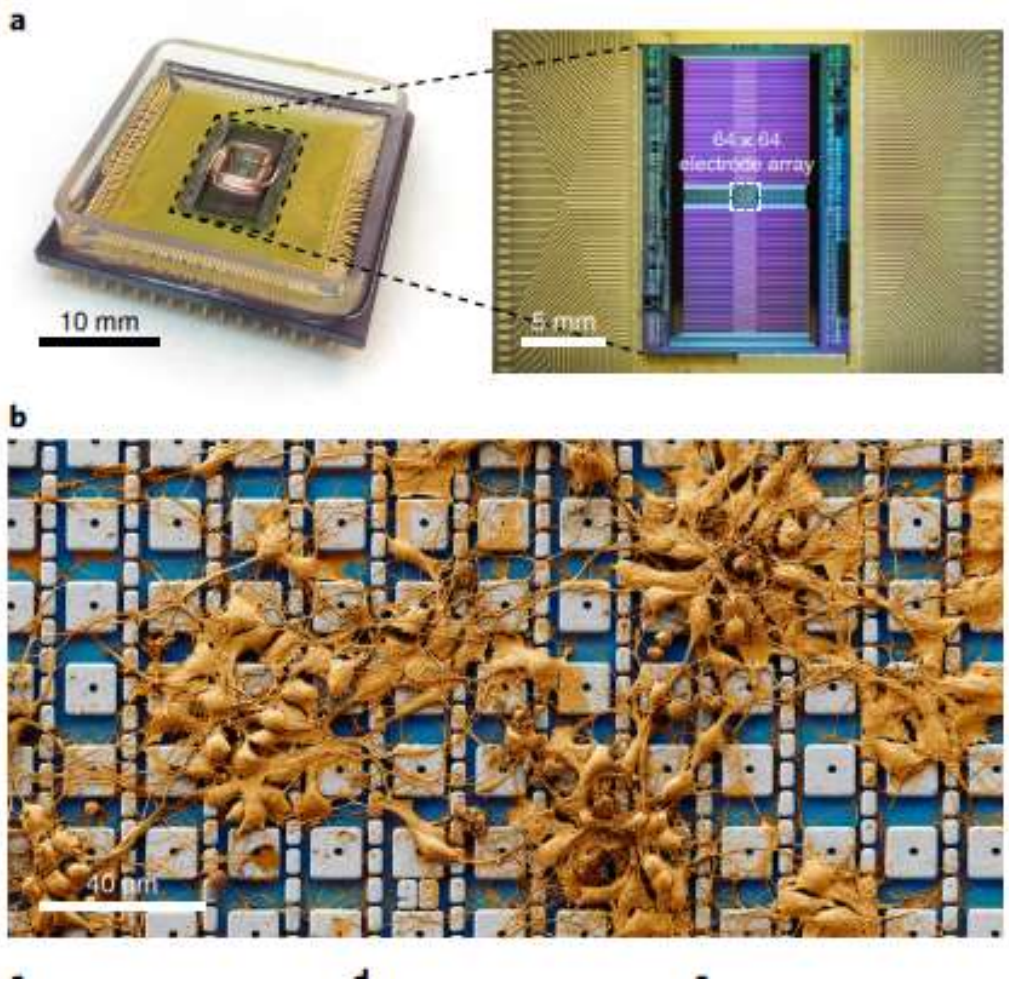

Abbott et al., (2020) Nature Biomedical Engineering, 4, 232–241

A novel **nanoelectrode MEA** has now been developed that can simultaneously record intracellularly from many thousands of connected neurones in cell culture. The array consists of 4096 Pt-black electrodes with nanoscale roughness fabricated on top of a silicon chip that integrates 64x64 microscale amplifiers, configured into pseudo-current clamp or pseudo-voltage clamp modes. Electrode current injection is used to permeabilize the cell membranes for i.c. access in pCC and pVC configurations.

Multielectrode arrays (MEAs)

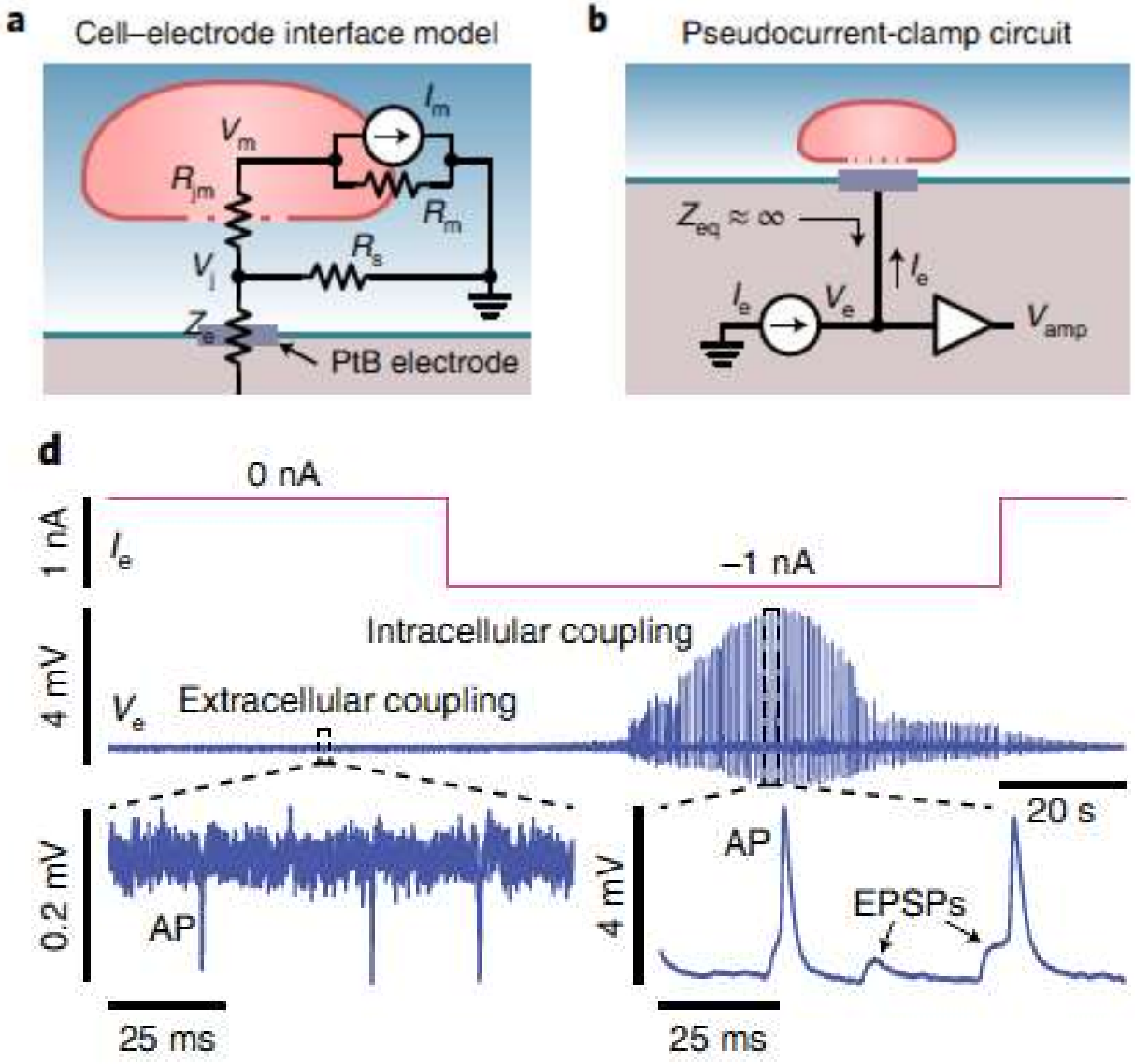

Abbott et al., (2020) Nature Biomedical Engineering, 4, 232–241

Intracellular recording and stimulation of dissociated rat neurones using the pCC configuration. a: model of the electrode–neurone interface. b, The pCC configuration consists of a current injector with output current I_e, and a high input impedance (Z_{eq}) voltage. d, Extracellular measurement of a neurone transitions to intracellular with -1 nA applied through the pixel in pCC. Spontaneous EPSPs and APs are now clearly visible.

How can one study the properties of individual synapses?

Double i.c./patch clamp recording

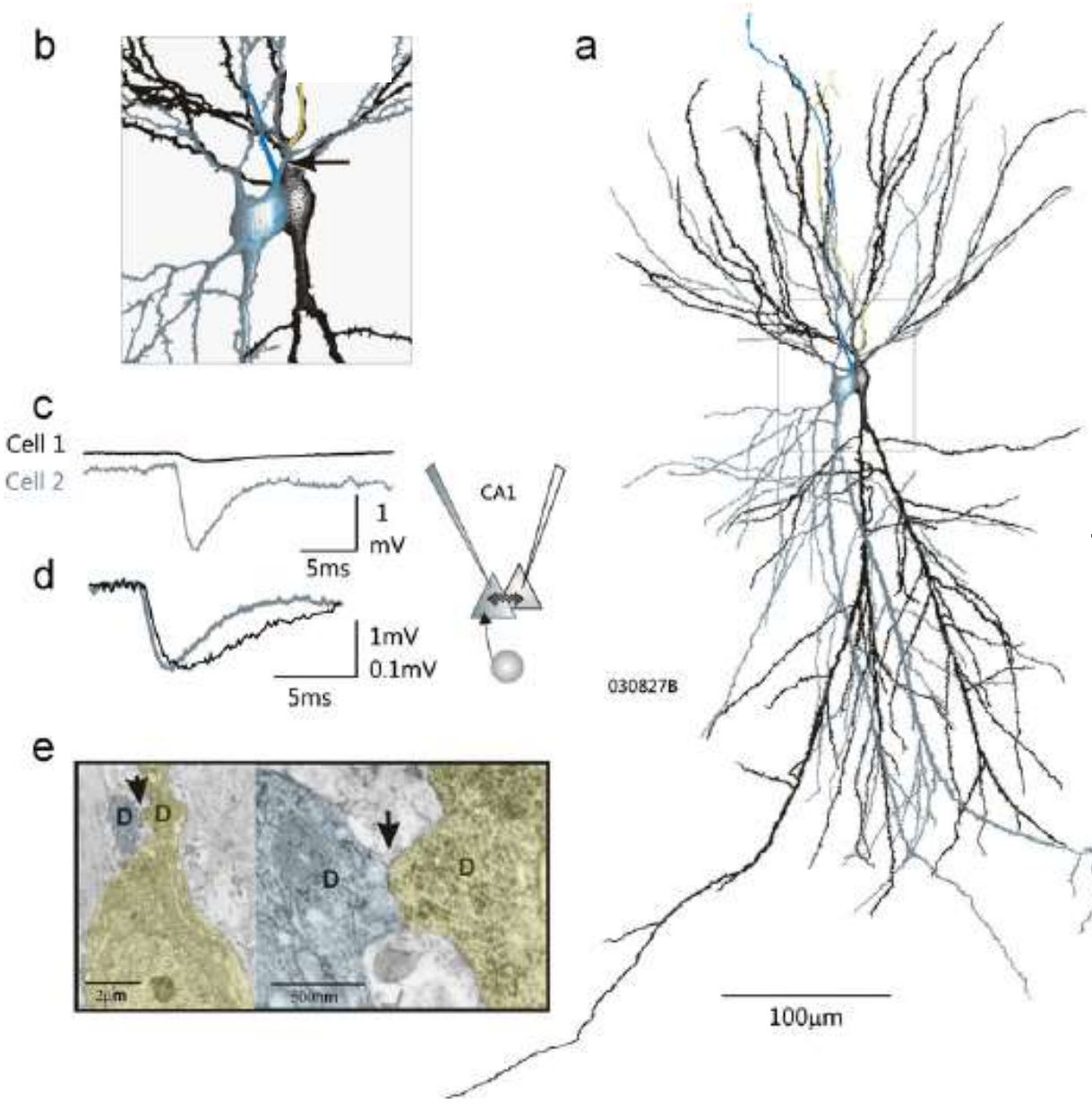

Over the years, detailed knowledge has been obtained about the nature of synaptic communication between central neurones by using **double 'sharp' intracellular or double patch clamp recording** followed by reconstruction and identification of the recorded neurones. Passive electrical transfer of synaptic events from one CA1 pyramidal cell to another electrically coupled pyramidal cell. (a) Reconstruction of the two pyramidal cells.

Mercer, (2012) Brain Research, 1487, 192-197.

Double i.c./patch clamp recording

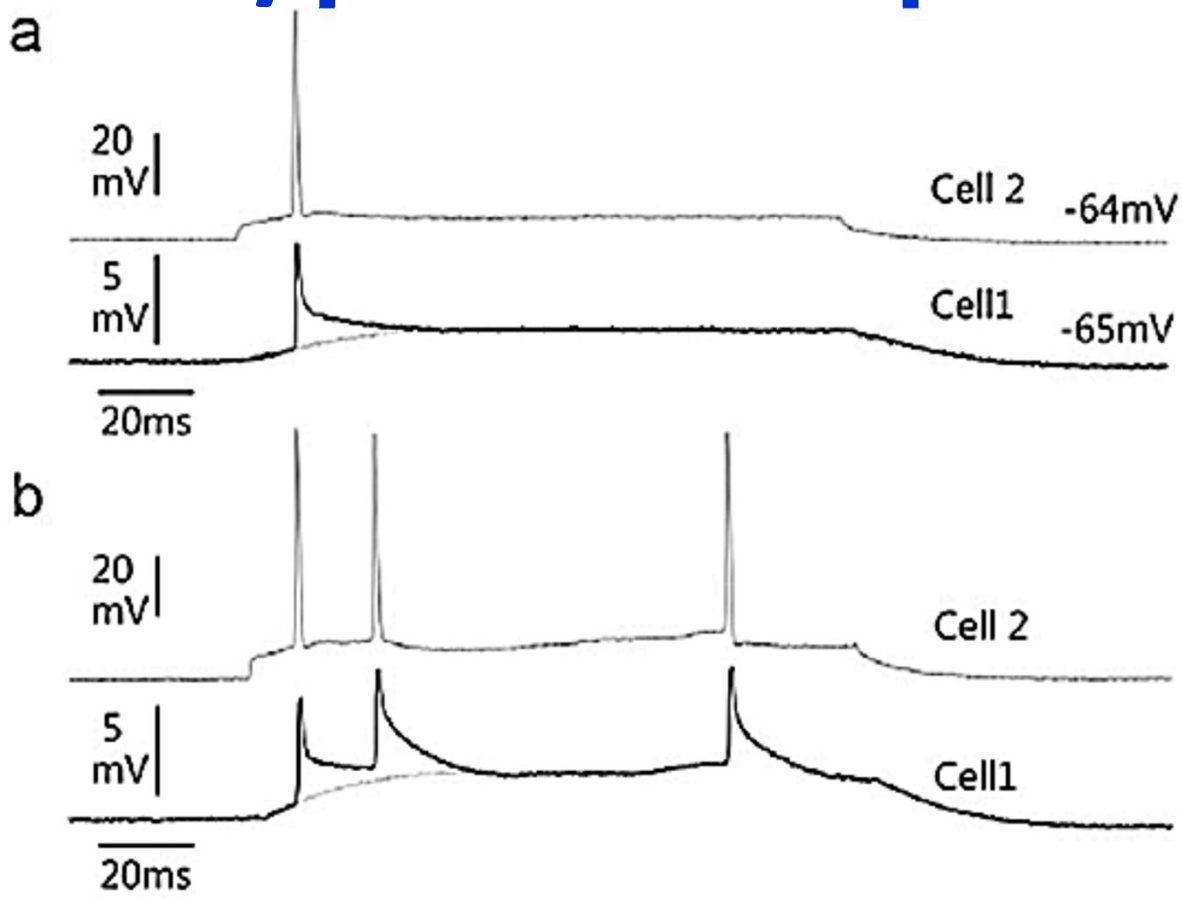

Action potentials in one **CA1 pyramidal cell** activate 'spikelets' in a coupled, follower cell which can elicit action potentials in that cell (a) and (b) Supra-threshold current pulses injected into Cell 2 generate APs that activate ' spikelets' in Cell 1.

Mercer, A. (2012) Brain Research, 1487, 192-197.


Take a
Break!

Are there ways to selectively stimulate or inhibit neurones ?

Optogenetics

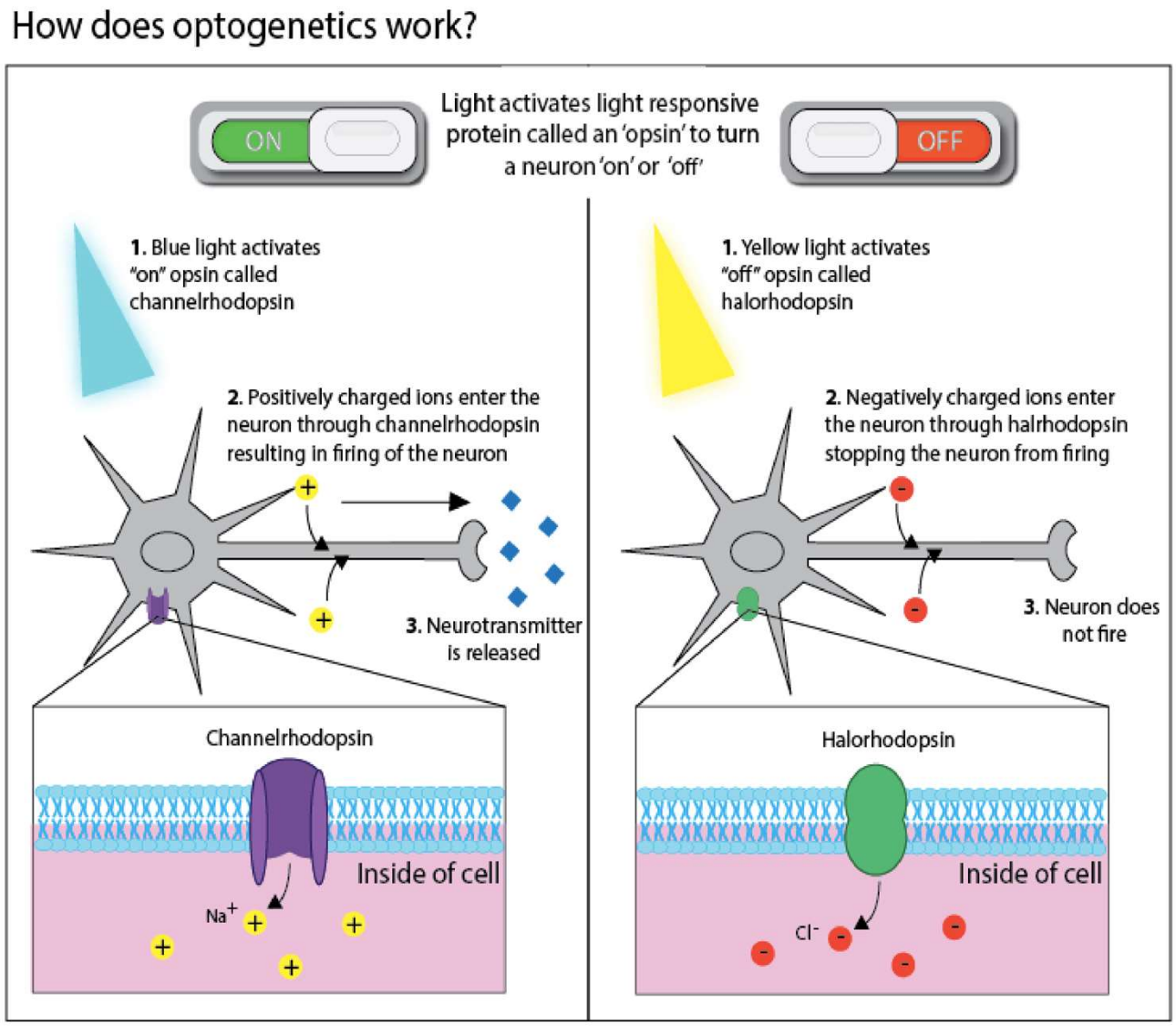

Optogenetics relies on light-responsive **opsins** to selectively turn neuronal activity on or off with a flash of light. **Channelrhodopsin-2,** is found in algae. When activated by blue light, channelrhodopsin lets Na^+/ Ca^{2+} ions enter the neurone, whereas **halorhodopsin**, lets Cl^- ions enter when activated with yellow light. By inserting the genes for these "on" and "off" opsins into mice, it is then possible to control their neuronal activity using blue or yellow laser light.

Optogenetics

How optogenetics works

A light-sensitive protein from algae

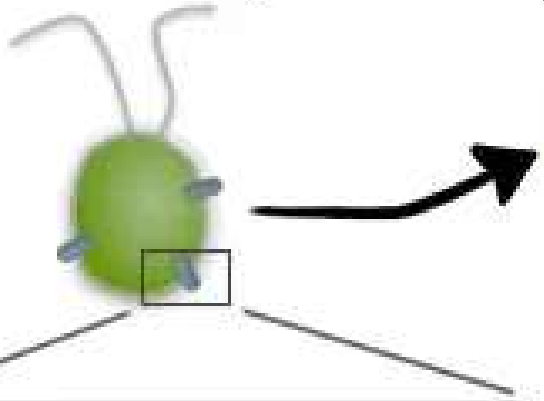

Take the gene for this protein...

... and insert the DNA into specific neurons in the brain

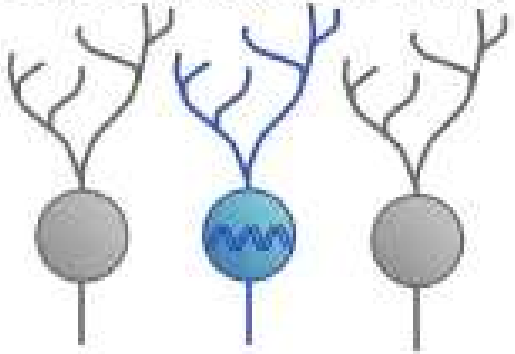

Neurons communicate by "**firing**." This is an electrical signal created by opening & closing ion channels.

This protein is an ion channel that opens in response to **blue light**

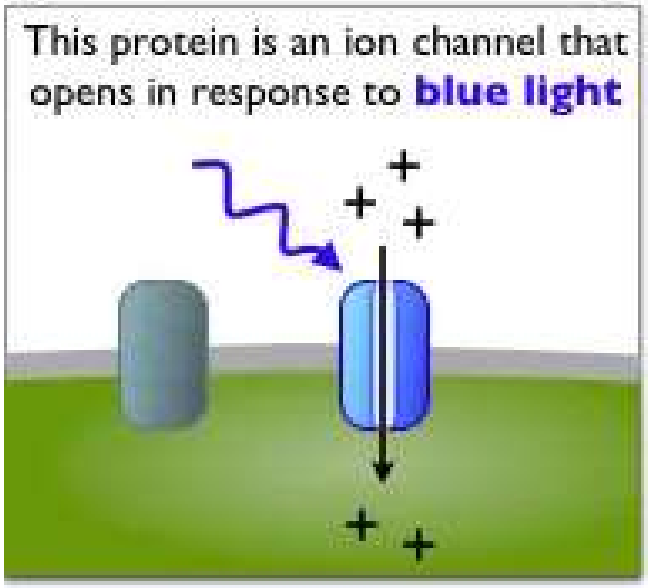

So now you can cause neurons to fire just by flashing **blue light!**

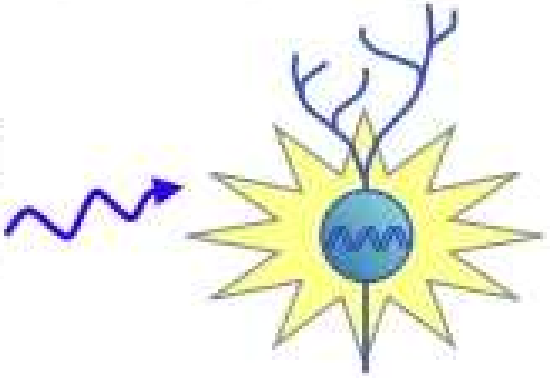

With the right combination of neurons, you can activate an entire brain circuit to control specific behaviors (like movement)

Optogenetics

Identification of reward circuit

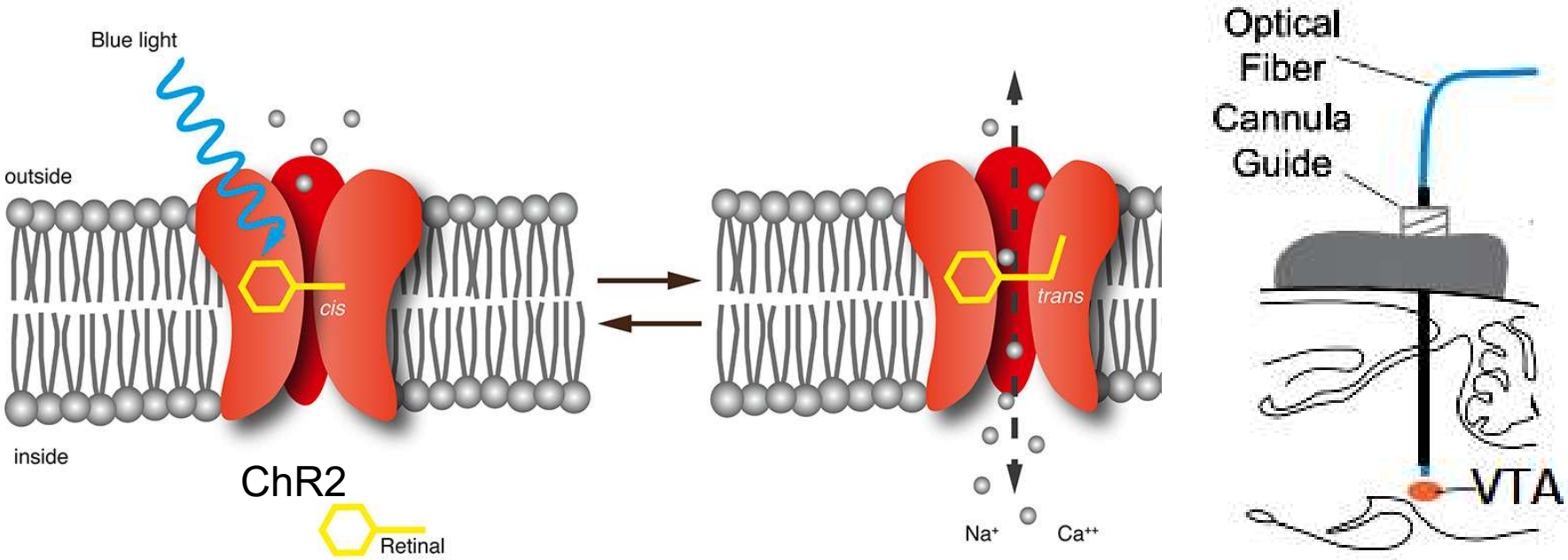

Recently, ***optogenetics*** using ***channelrhodopsin-2 (ChR2)*** has been employed in order to selectively stimulate DA neurones in the VTA using a surgically implanted cannula carrying blue light laser illumination via an optical fibre.

Pascole et al., (2015) Neuron, 88(5), 1054-1056.

Optogenetics

Reward: blue light-self-administration

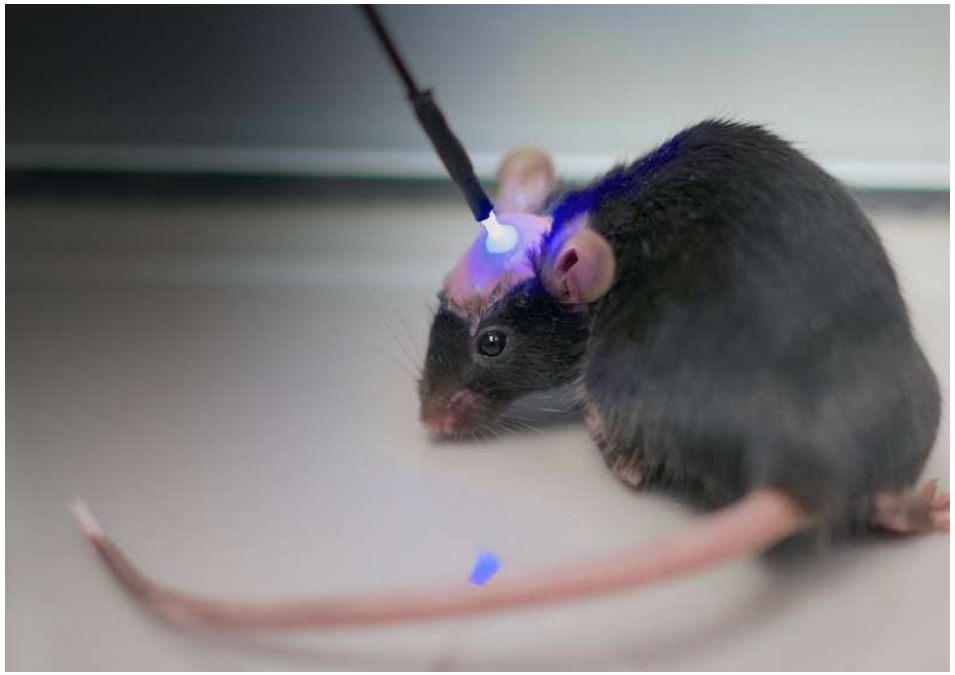

Animals are then trained to press a lever to self-administer the laser light stimulus. Following illumination with blue light (activation maximum 470 nm), ChR2 channels previously expressed selectively in the VTA DA neurones allow the entry of cations (mostly Na^+ and Ca^{2+}) into the cells, causing depolarization and DA release in the Nucleus Accumbens in a similar manner to electrical stimulation.

Pascole et al., (2015) Neuron, 88(5), 1054-1056.

Is it possible to visualise exocytotic release of neurotransmitters from cells?

Capacitance measurements/amperometry

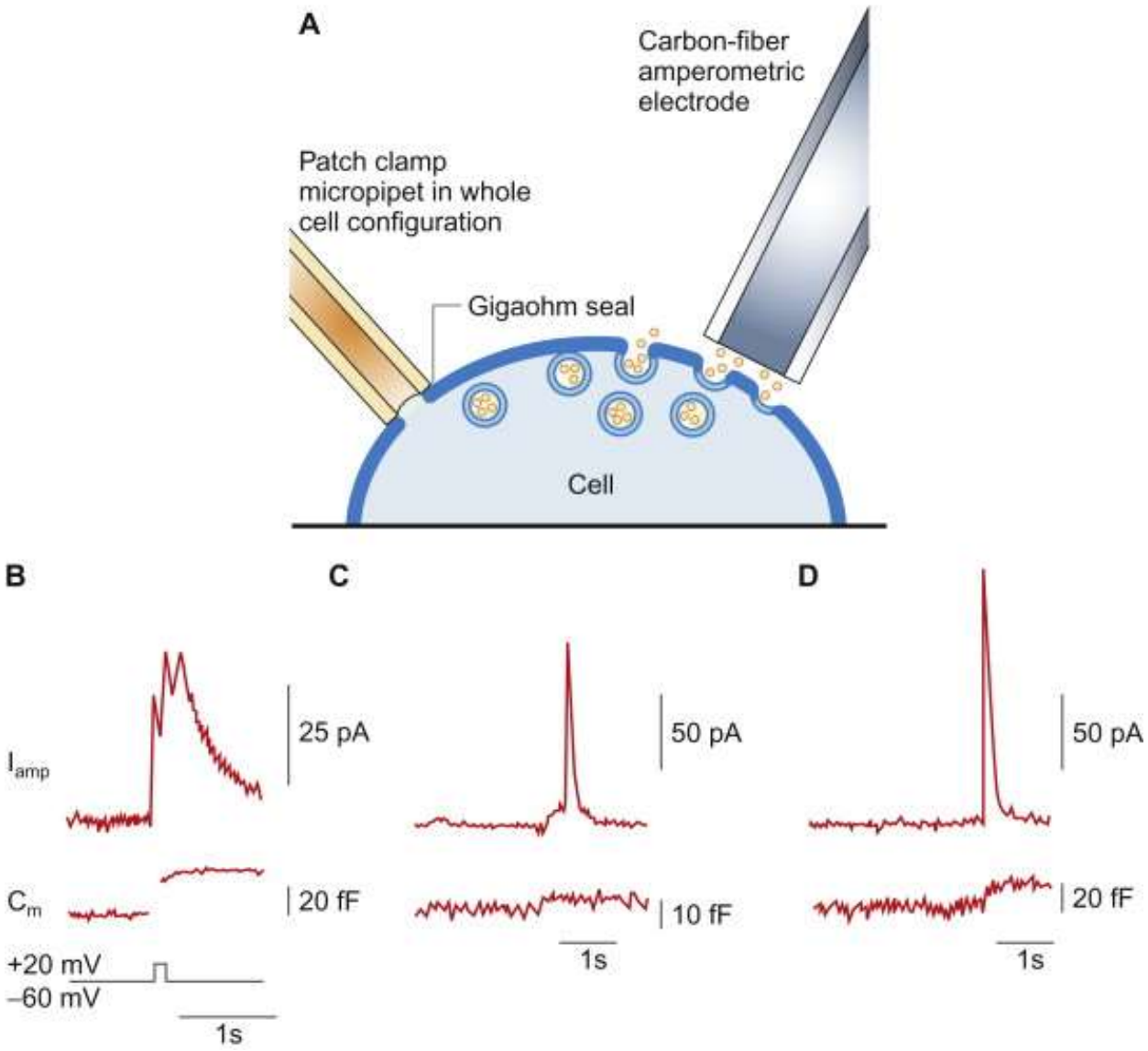

Secretory events monitored by simultaneous amperometric (Iamp) and capacitance (Cm) measurements in a patch-clamped **adrenal chromaffin cell.** (A) Configuration of the recording setup. (B) Amperometric response with multiple spikes due to the fusion of several secretory vesicles triggered by a 50 ms depolarization to +20 mV from −60 mV. The capacitance response reflects the fusion of several or single vesicles with the plasmalemma.

Robinson et al., (1995) Proc.Nati.Acad.Sci.USA 92, 2474-2478

Is it possible to visualise intracellular Ca^{2+} changes in neurones?

Ca^{2+} imaging

- **Ca^{2+} ions** can generate a variety of important intracellular signals that control key functions in all types of neurones. Over the years, various methods have been developed for imaging Ca^{2+} changes in neurones **in real time** using a range of Ca^{2+}- sensitive dyes in conjunction with sophisticated Ca^{2+} imaging devices, including confocal and two-photon microscopes.
- Techniques have now advanced to the point where it is possible to map neuronal Ca^{2+} changes in in awake, behaving animals as well as in single sensory dendritic spine inputs in cortical neurones *in vivo*.

For review see: Grienberger and Konnerth (2012) Imaging Calcium in Neurons Neuron 73, 862-885.

Ca^{2+} imaging

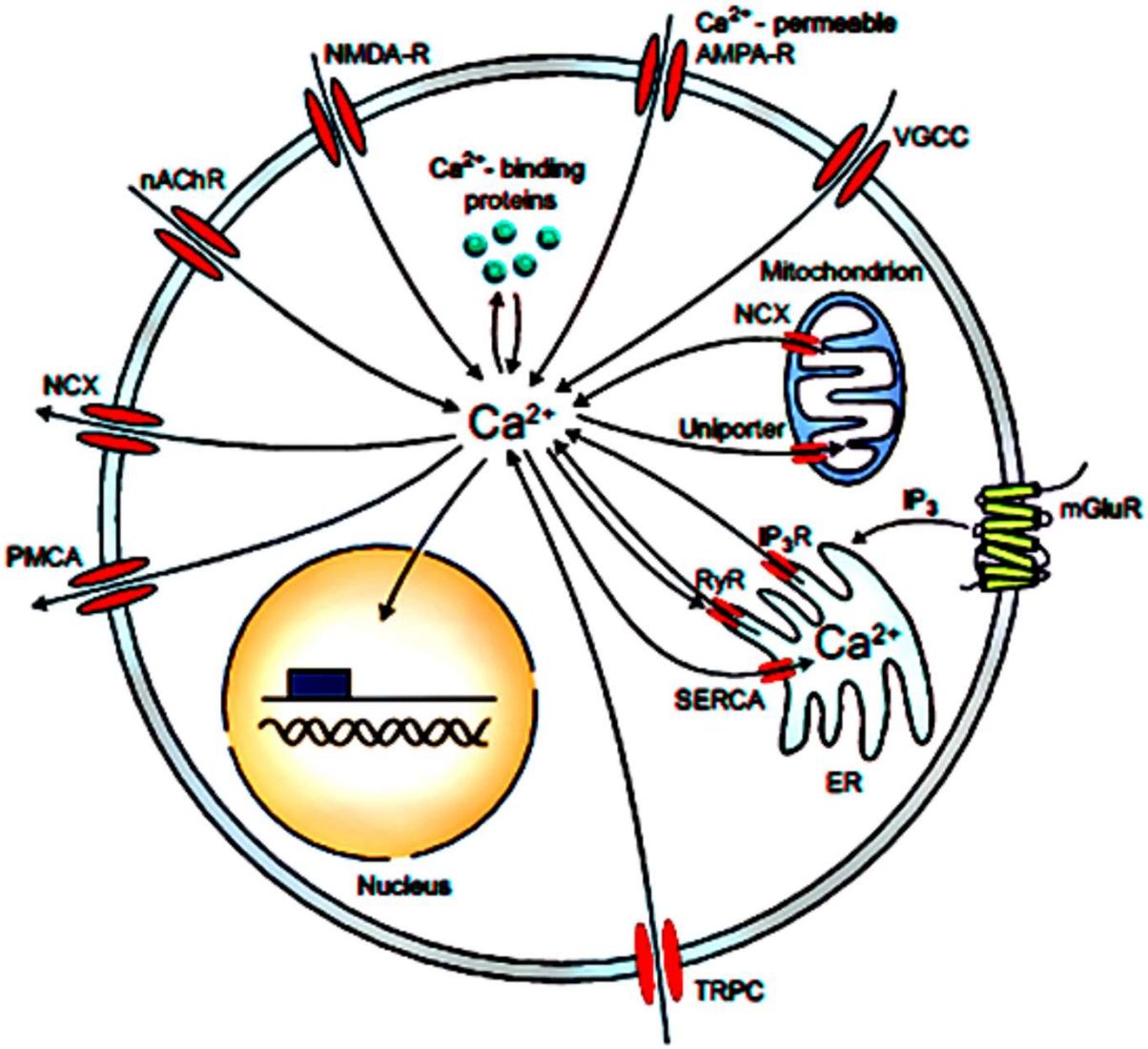

Sources of calcium influx are Ca^{2+} channels (VGCCs), calcium-permeable AMPA and NMDA glutamate receptors, nAChRs, and transient receptor potential type C (TRPC) channels. Ca^{2+} release from internal stores is mediated by IP_3Rs and RyRs. IP_3 can be generated by mGluRs. Ca^{2+} efflux is mediated by the plasma membrane calcium ATPase (PMCA),sodium-calcium exchanger (NCX), and sarco-/endoplasmic reticulum calcium ATPase (SERCA). Mitochondria are also important for Ca^{2+} homeostasis

Ca^{2+} imaging

Table 1. Frequently Used Fluorometric Calcium Indicators

Name	Kd (nM)	Examples of In Vivo Applications	Representative References
Chemical Calcium Indicators			
Oregon Green BAPTA-1	170	Mouse neocortex, mouse hippocampus, mouse olfactory bulb, rat neocortex, rat cerebellum, ferret neocortex, cat neocortex, zebrafish	Dombeck et al., 2010; Sullivan et al., 2005; Ohki et al., 2005; Li et al., 2008; Greenberg et al., 2008; Rochefort et al., 2011; Sumbre et al., 2008; Wachowiak et al., 2004
Calcium Green-1	190	Mouse neocortex, mouse olfactory bulb, honeybee, turtle, zebrafish, rat neocortex	Dombeck et al., 2009; Oka et al., 2006; Galizia et al., 1999; Wachowiak et al., 2002; Brustein et al., 2003; Svoboda et al., 1997
Fura-2	140	Mouse neocortex	Sohya et al., 2007
Indo-1	230	Mouse neocortex	Stosiek et al., 2003
Fluo-4	345	Mouse neocortex, Xenopus larvae	Sato et al., 2007; Demarque and Spitzer, 2010
Rhod-2	570	Mouse neocortex, Zebrafish	Takano et al., 2006; Yaksi et al., 2009
X-rhod-1	700	Mouse neocortex	Nagayama et al., 2007

Ohara et al., (2009) The Neuroscientist 15 (5) 450-463

Ca^{2+} imaging

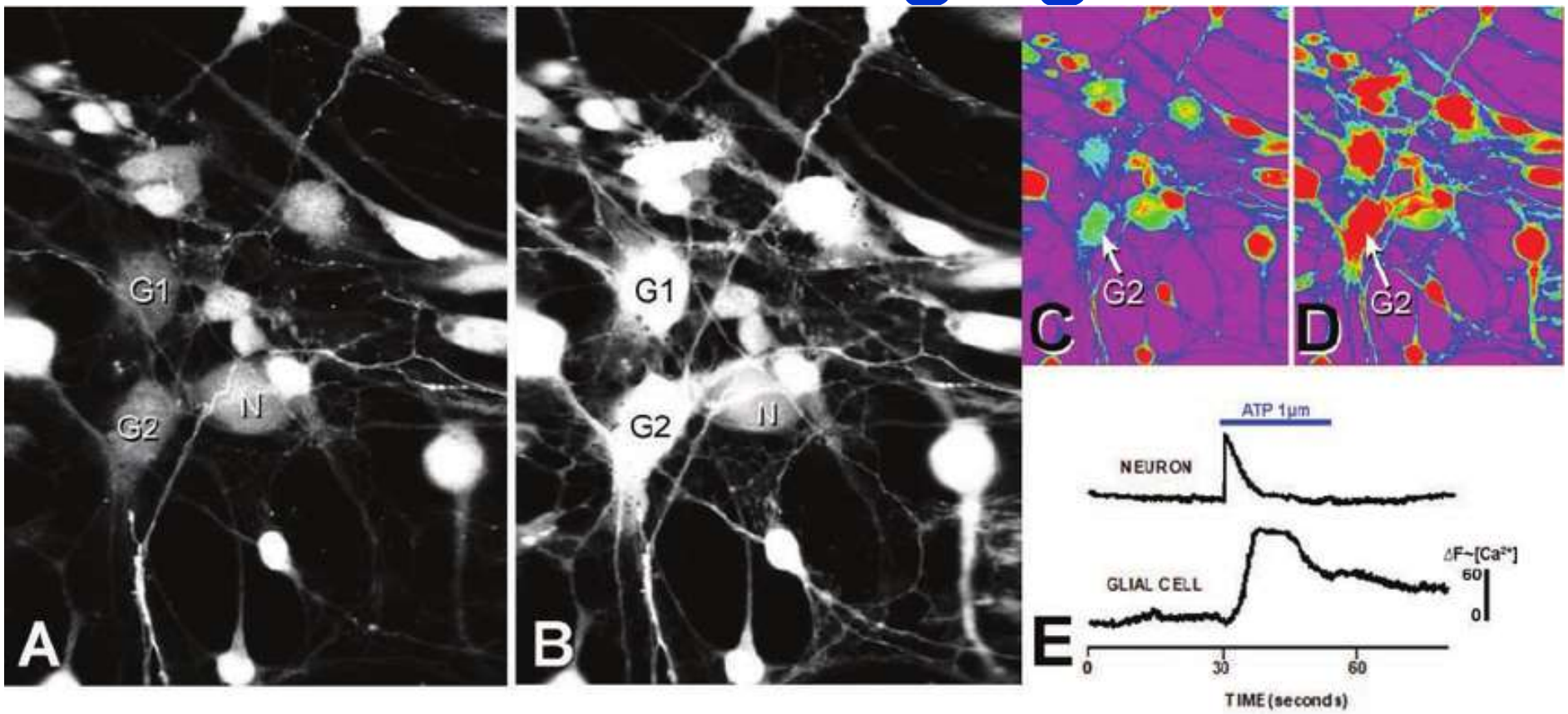

Calcium imaging of dissociated neurones and glia from the **trigeminal ganglion**. Dissociated trigeminal neurons (N) and glial cells (G1, G2) loaded with the **fluorescence calcium indicator Fluo-4-AM** are shown before (A) and after (B) addition of 1 µM of ATP. C,D Pseudocolour representation of the calcium intensity of A and B. Green indicates low and red indicated high calcium concentration. (E) Differences in the time course of calcium influx between a neurone and a glial cell after ATP application.

∗ ΔF/F ={ F(t) - F0)/F0 }

Ca^{2+} imaging

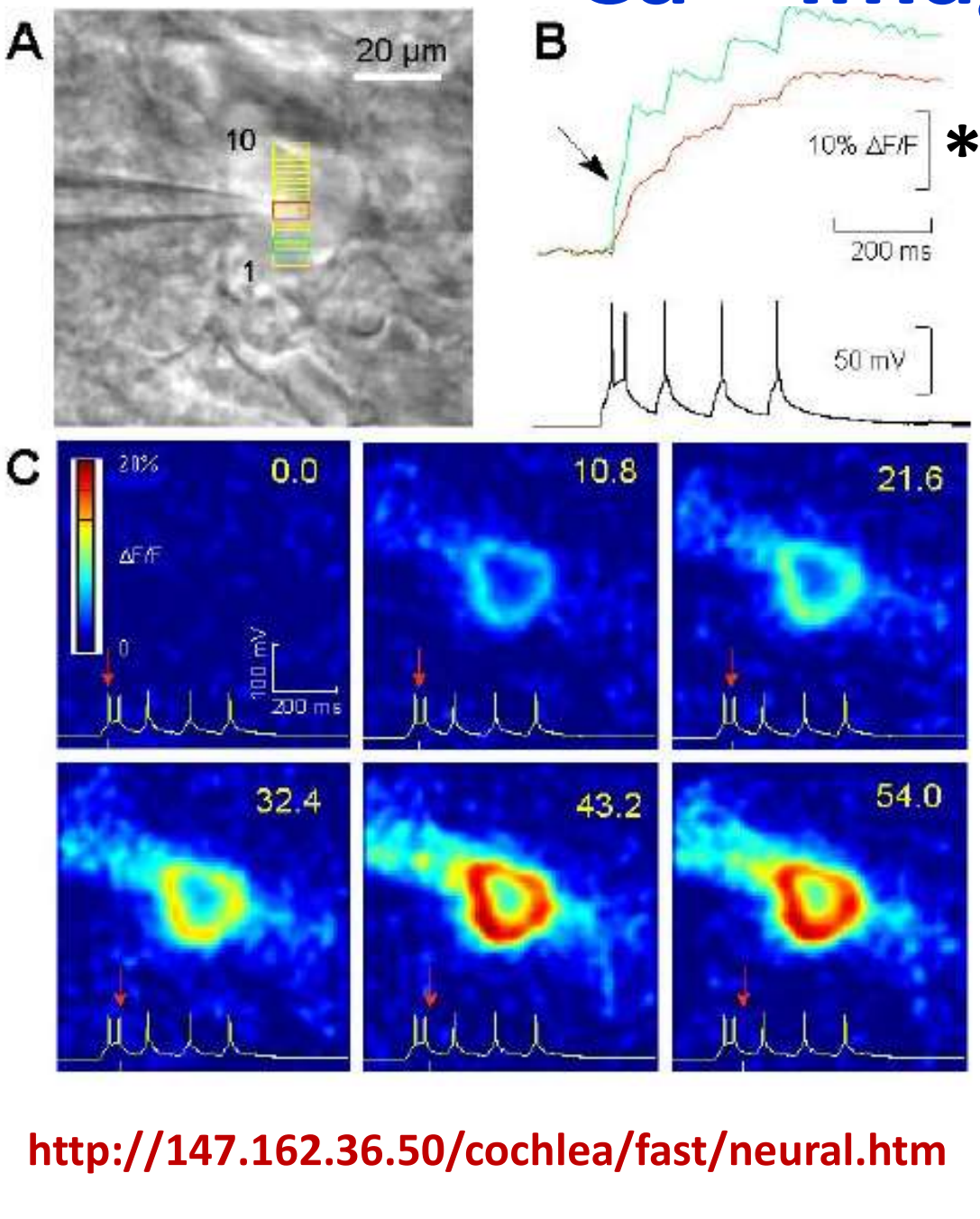

http://147.162.36.50/cochlea/fast/neural.htm

Intracellular [Ca $^{2+}$]i imaging in a **rat hippocampal CA3 pyramidal neurone** in a 200 µm-thick brain slice. (A) A patch pipette is used to load the cell with **75 µM Calcium Green-1**. (B) Simultaneous recordings of membrane potential and mean fluorescence change from the red and green ROIs in (A). Somatic injection 30 ms 200 pA pulses evokes action potentials and cumulative calcium entry identifiable from change in ΔF/F measured at the cell boundary. (C) Frames at 10.8 ms (93 frames/s) show change in Ca^{2+} fluorescence.

Ca^{2+} imaging

GECI's

Genetically Encoded Calcium Indicators			
Camgaroo 1		Drosophila	Yu et al., 2003
Camgaroo 2		Drosophila, mouse olfactory bulb	Yu et al., 2003; Hasan et al., 2004
Inverse pericam	200	Zebrafish, mouse olfactory bulb	Hasan et al., 2004; Li et al., 2005
GCaMP 2	840	Mouse olfactory bulb, mouse cerebellum	Fletcher et al., 2009; Diez-Garcia et al., 2005
GCaMP 3	660	Mouse neocortex, mouse hippocampus, Drosophila, C. elegans	Tian et al., 2009; Dombeck et al., 2010; Seelig et al., 2010; Tian et al., 2009
Yellow Cameleon 3.6	250	Mouse neocortex	Lütcke et al., 2010
Yellow Cameleon Nano	15–50	Zebrafish	Horikawa et al., 2010
D3cpV	600	Mouse neocortex	Wallace et al., 2008
TN-XL	2200	Drosophila, macaque	Mank et al., 2006; Heider et al., 2010
TN-L15	710	Mouse neocortex	Heim et al., 2007
TN-XXL	800	Drosophila, mouse neocortex	Mank et al., 2008; Mank et al., 2008

In recent years, **GECIs** have become a widely used tool in neuroscience whereby a range of Ca^{2+-} sensitive fluorescent proteins can be expressed genetically in selected neurones using viral transduction. The viral construct with the GECI can be targeted to specific brain areas by means of stereotaxic injection in order to visualise the cells of interest.

Siciliano & Tye (2019) Alcohol 74, 47-63

Ca^{2+} imaging

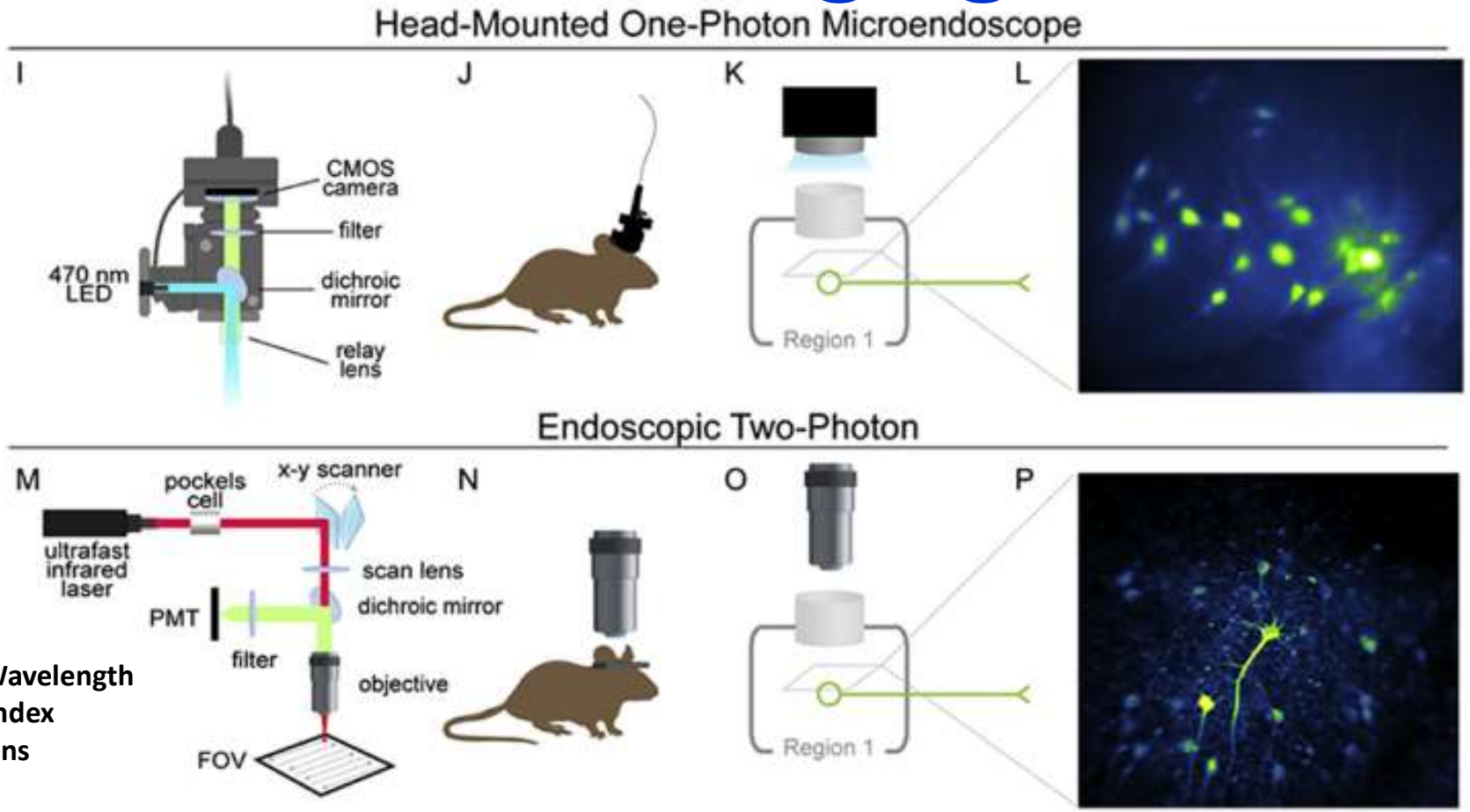

Single Wavelength Graded-Index (GRIN) Lens

Miniature head-mounted one-photon microscope is attached to the animal via a magnetic baseplate to visualize **GECI-expressing cells** during free behaviour. A chronically implanted GRIN lens allows optical access to a deep-brain region containing GECI-expressing cells shown in L. (M) Two-photon microscopy. Pulses of infrared light through an objective, scan the head-fixed under the microscope.

Model cell systems

- Sometimes it is useful to be able to study the behaviour of ion channels and receptors in a more convenient cell model system. Over the years, such systems have developed to the point where they have largely replaced *in vitro* brain slices or cell culture methods for conducting detailed neuroscience investigations.
- The classical “model cell” system is the ***Xenopus* oocyte**, originally pioneered by Ricardo Miledi’s laboratory in which specific mRNA or cDNA was injected into oocytes which then expressed the required ion channel/receptor in the cell membrane, allowing electrophysiological analysis to be carried out using conventional two electrode voltage clamp techniques.

Model cell systems

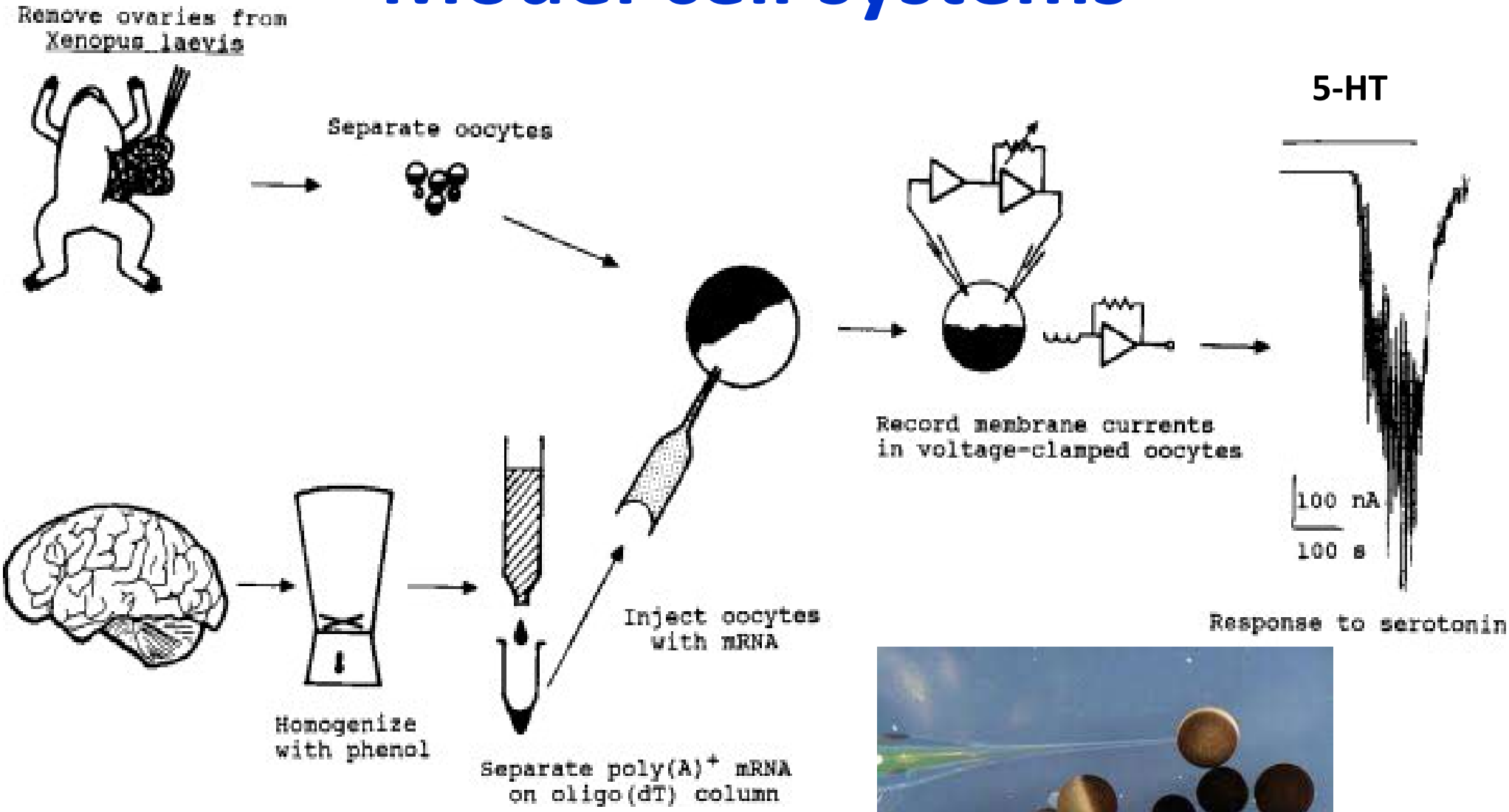

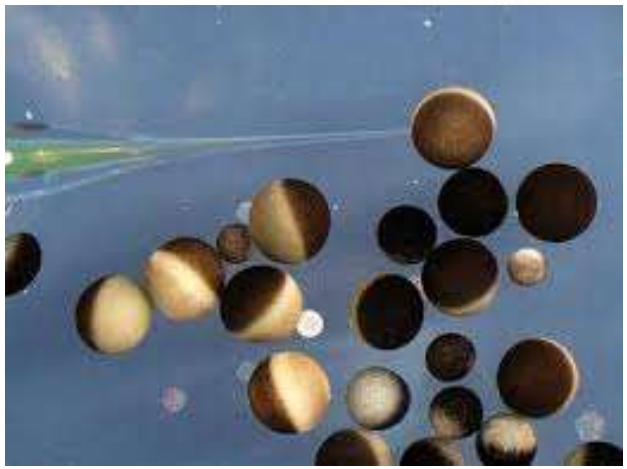

Model cell systems

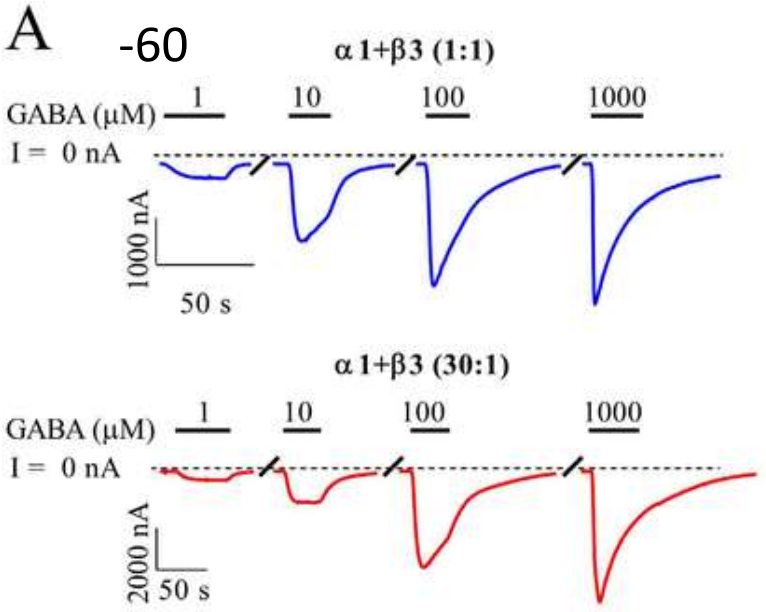

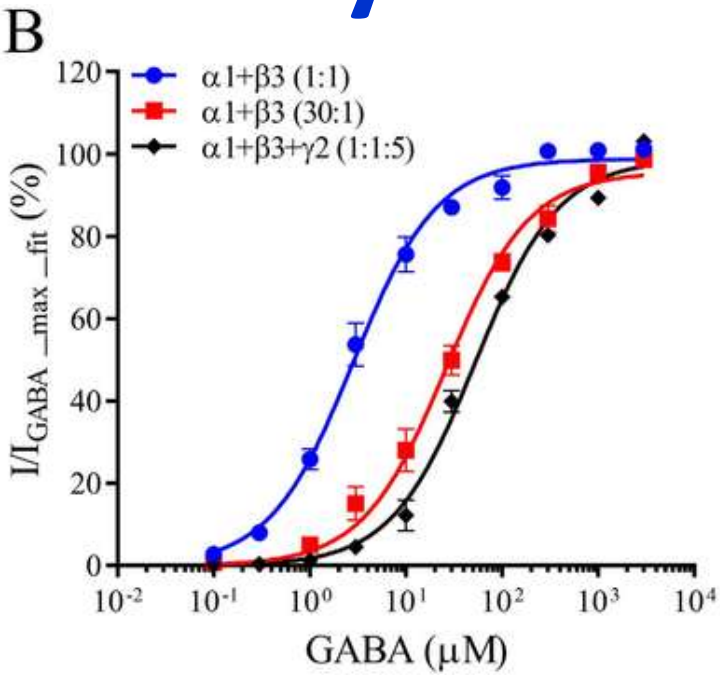

GABA-evoked responses at α1β3 and α1β3γ2 $GABA_A$ receptors. *Xenopus laevis* oocytes were injected with cRNA and subjected to two-electrode voltage-clamp.

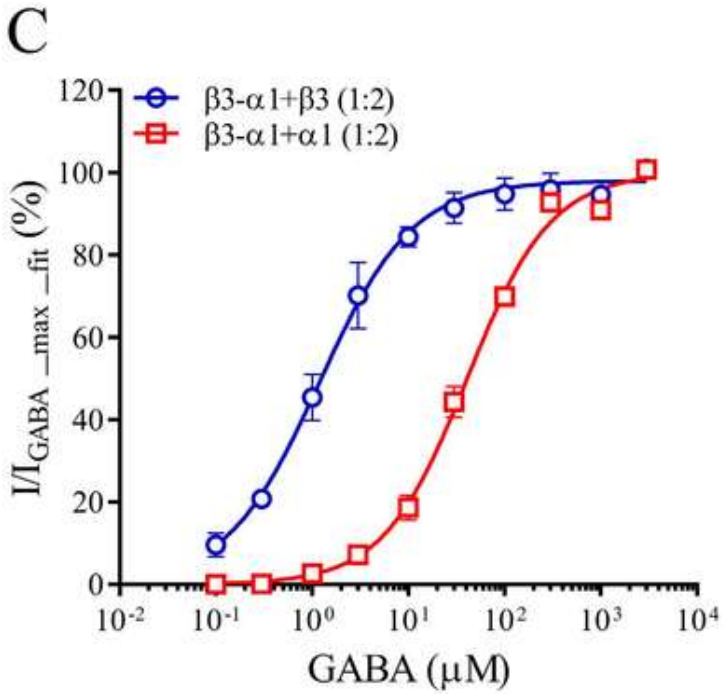

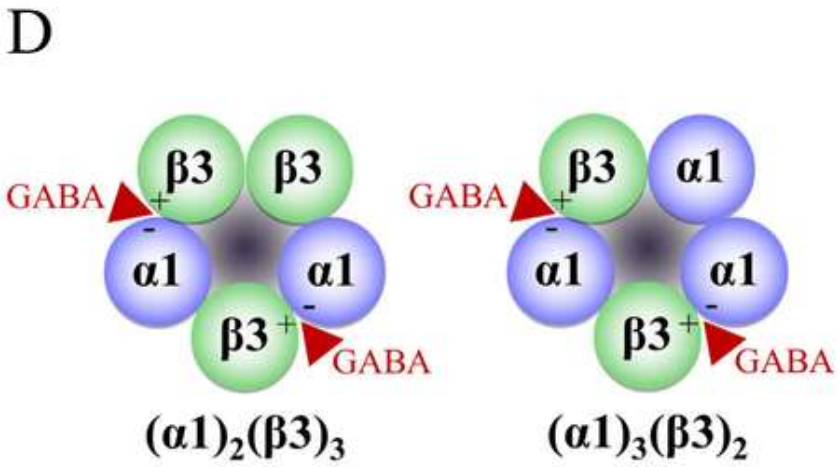

Tarmizi et al., (2016) Science Report 6:28674.

Model cell systems

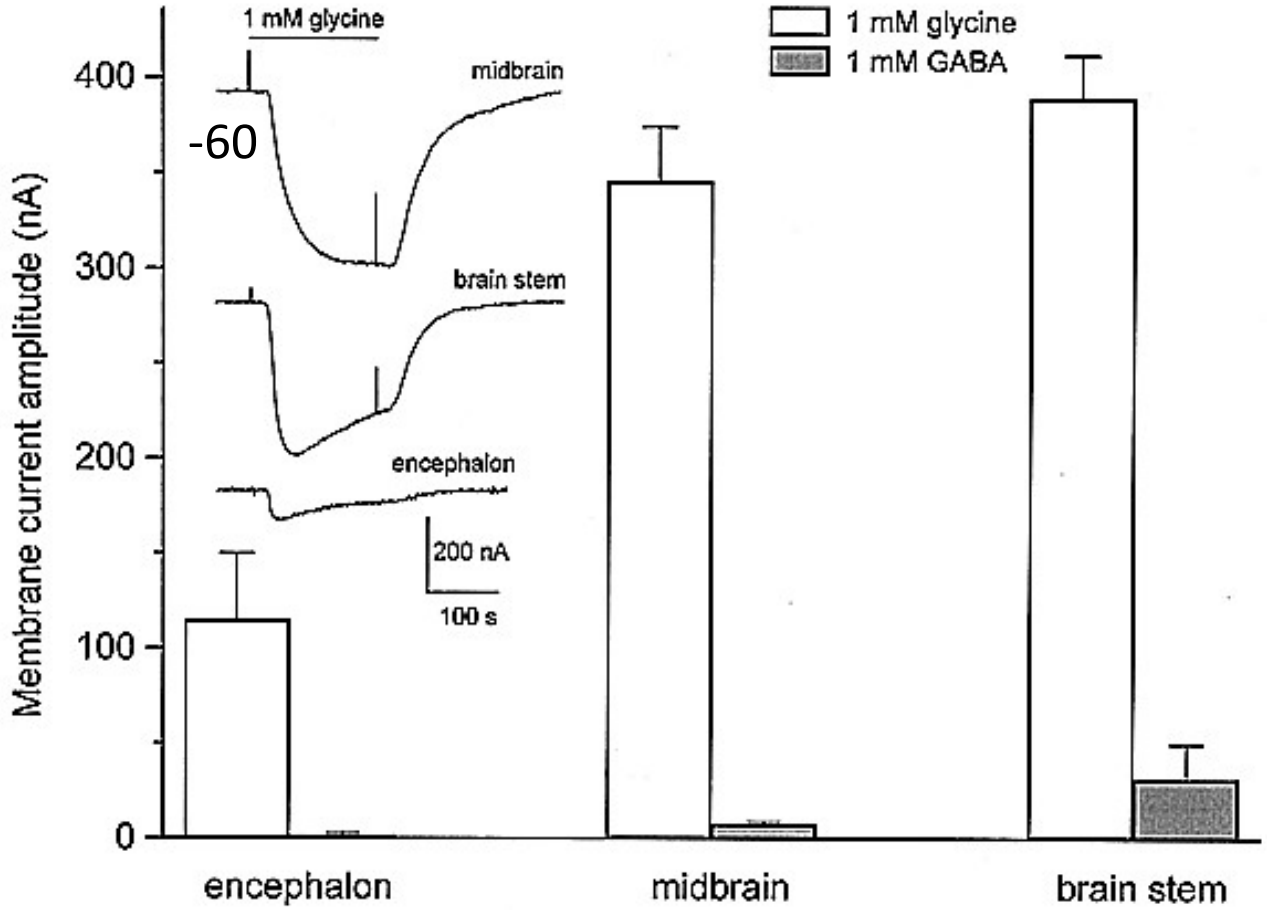

Expression of Glycine and GABA receptors by embryonic mRNAs. The columns represent the amplitude of membrane currents elicited by Glycine or GABA (1 mM) in oocytes injected with mRNA from 18-day-old rat embryo encephalon, midbrain, or brainstem. (Inset) Representative Glycine-currents. García-Alcocer et al., (2001) PNAS 98 (5) 2781-2785

Model cell systems

- Nowadays, it is more convenient to use readily available stable cell lines such as **HEK-293** (immortalized human embryonic kidney), **HeLa** (immortalised human cervical cancer) or **CHO** (Chinese hamster ovary) or cells with various transfection techniques to express channels/receptors of interest particularly when specific mutations or subunit combinations of ion channels/receptors are to be studied using standard patch clamp.
- Some other neural cell models include: **SK-N-SH** cells (neuroblastoma), **bEnd.3** cells (endothelial polyoma from cerebral cortex), **SHSY5Y** cells (neuroblastoma) and **Human Neural Stem Cells** (hNSCs).

Karra & Dahm (2010) Transfection Techniques for Neuronal Cells Journal of Neuroscience, 30 (18) 6171-6177.

Model cell systems

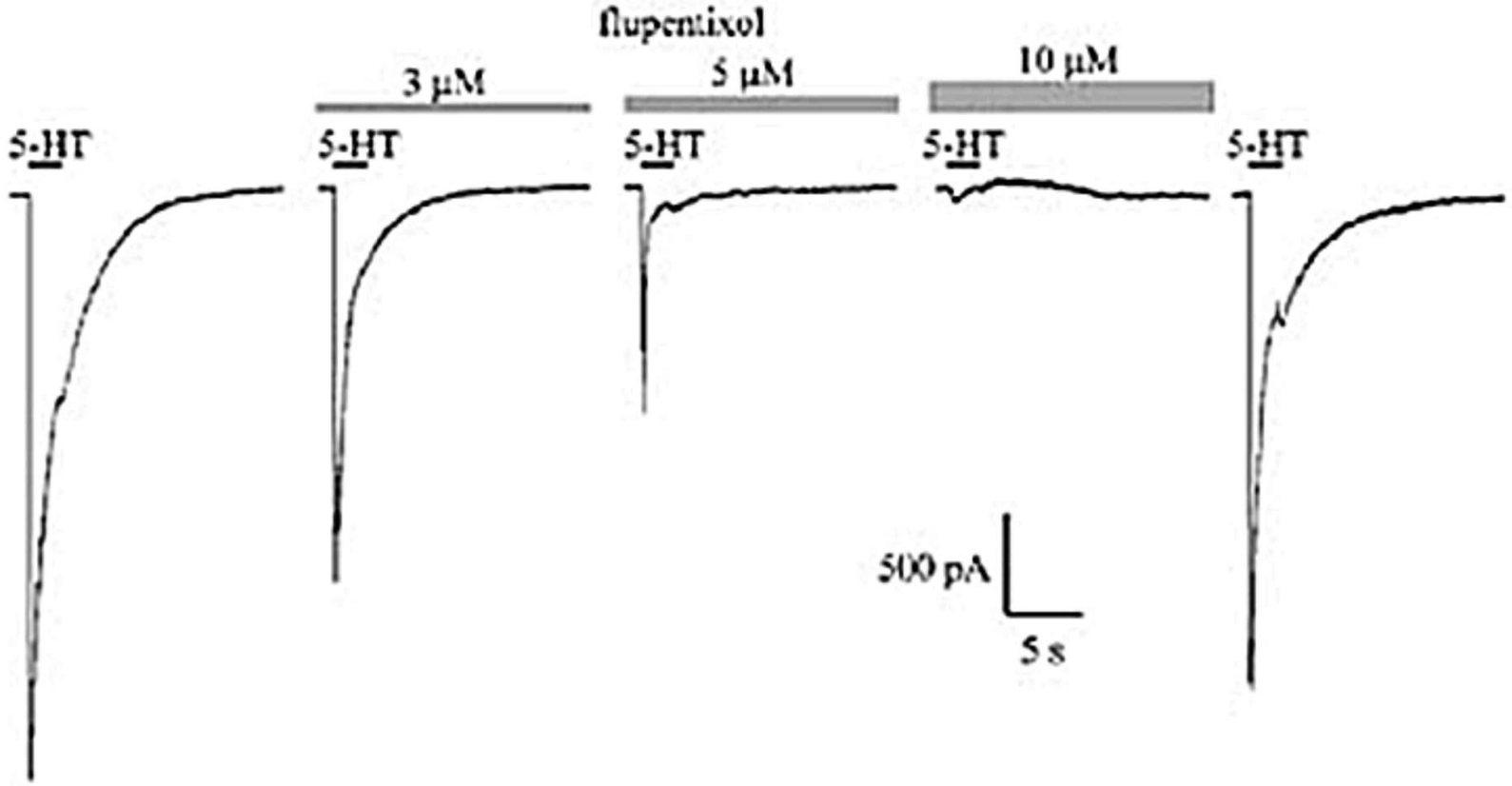

Concentration–response relationship of the effects of flupentixol on 5-HT-evoked cation currents in **HEK-5-HT3$_A$ cells**. Representative traces for the control and the recovery currents as well as for the effects of different concentrations of **flupentixol** (antipsychotic) on 5-HT3A-mediated currents. The application duration of 5-HT (10 µM) was 2 s.

Rammes et al., (2004). Molecular Psychiatry, 9, 846–858 .

Caged neurotransmitters for precision release: RuBi-Glutamate/RuBi-GABA

What are caged compounds?

- Caged compounds are specifically designed molecules whose structure is controlled by light. In the “caged” mode, the neurotransmitter of interest (*e.g.* glutamate/GABA) is pharmacologically inactivated by being bound to a “cage” moiety.
- Using a brief flash of visible or infrared light, this bond can be broken (“uncaged”) to release the active caged neurotransmitter at a discrete location depending on the experiment being conducted. Using this light activation method, enables experimenters to have full control over the timing, location and amplitude of neurotransmitter release at a defined site.

RuBi-Glutamate

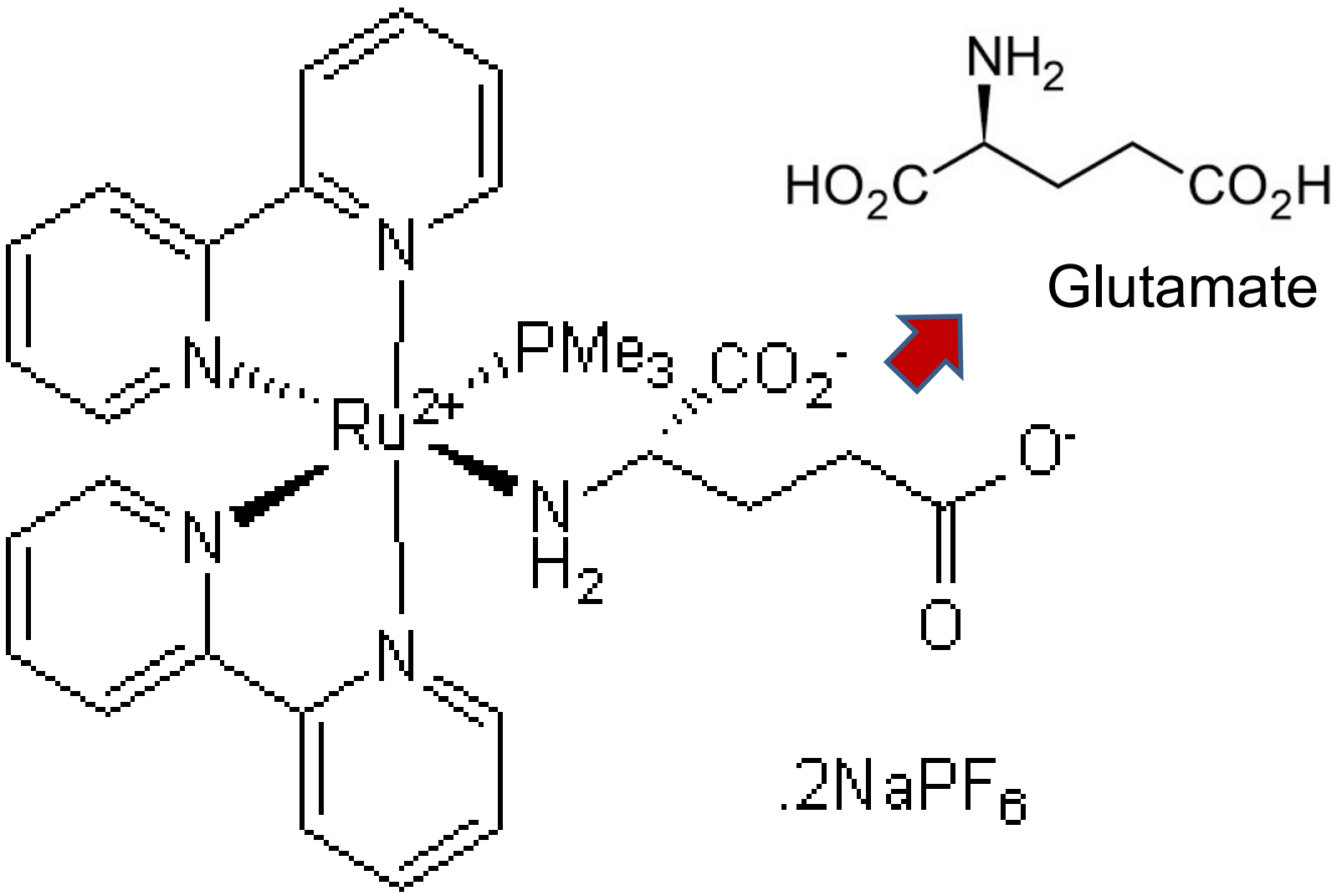

Ruthenium-bipyridine-trimethylphosphine caged glutamate

RuBi-Glutamate

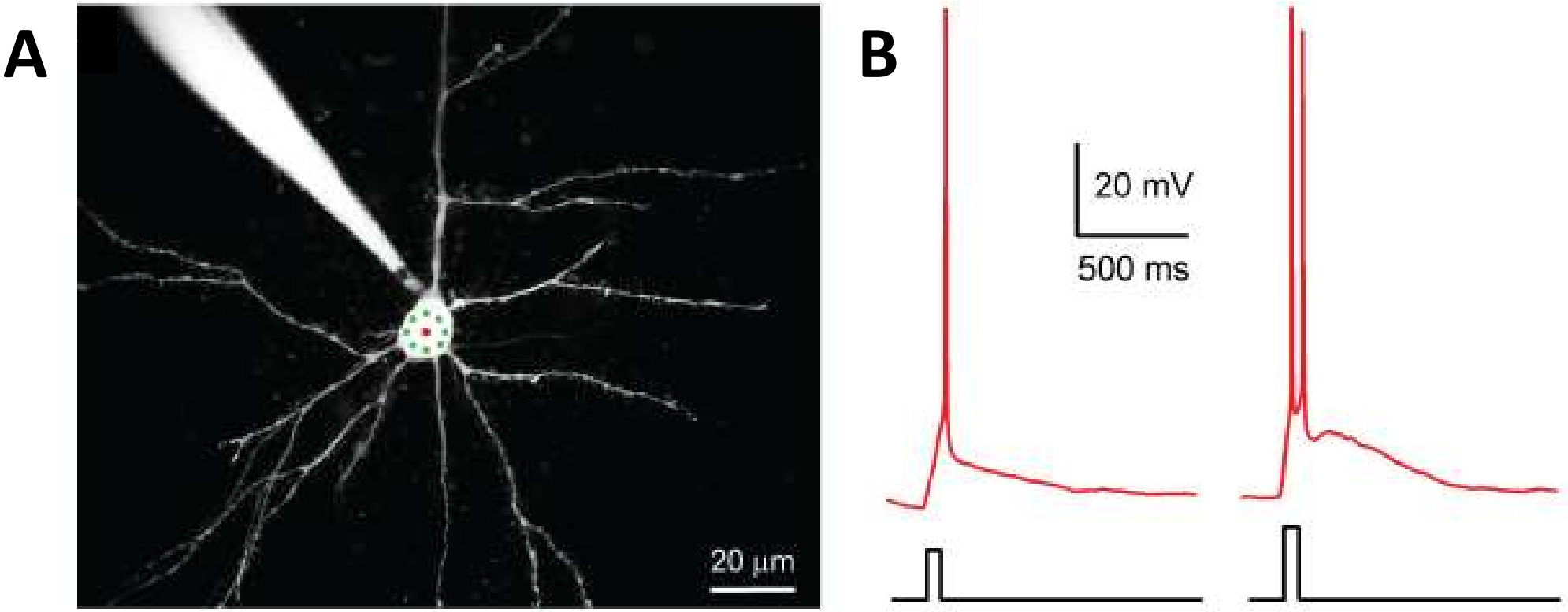

Glutamate photorelease from Rubi-Glutamate (300 µM in the bath). (A) Mouse cortical layer 2/3 pyramidal neurone loaded with **Alexa Fluor 594** and position of the multiplexed uncaging laser targets (eight subtargets) on the cell soma. (B) aEPSPs and action potentials triggered by two **near infra-red (800 nm)** twin photon uncaging of RuBi-Glutamate: one action potential was evoked with a 180 mW and two with a 220 mW laser pulse.

Fino et al., (2009). Front Neural Circuits 3:2. DOI: 10.3389/neuro.04.002.2009.

RuBi-Glutamate

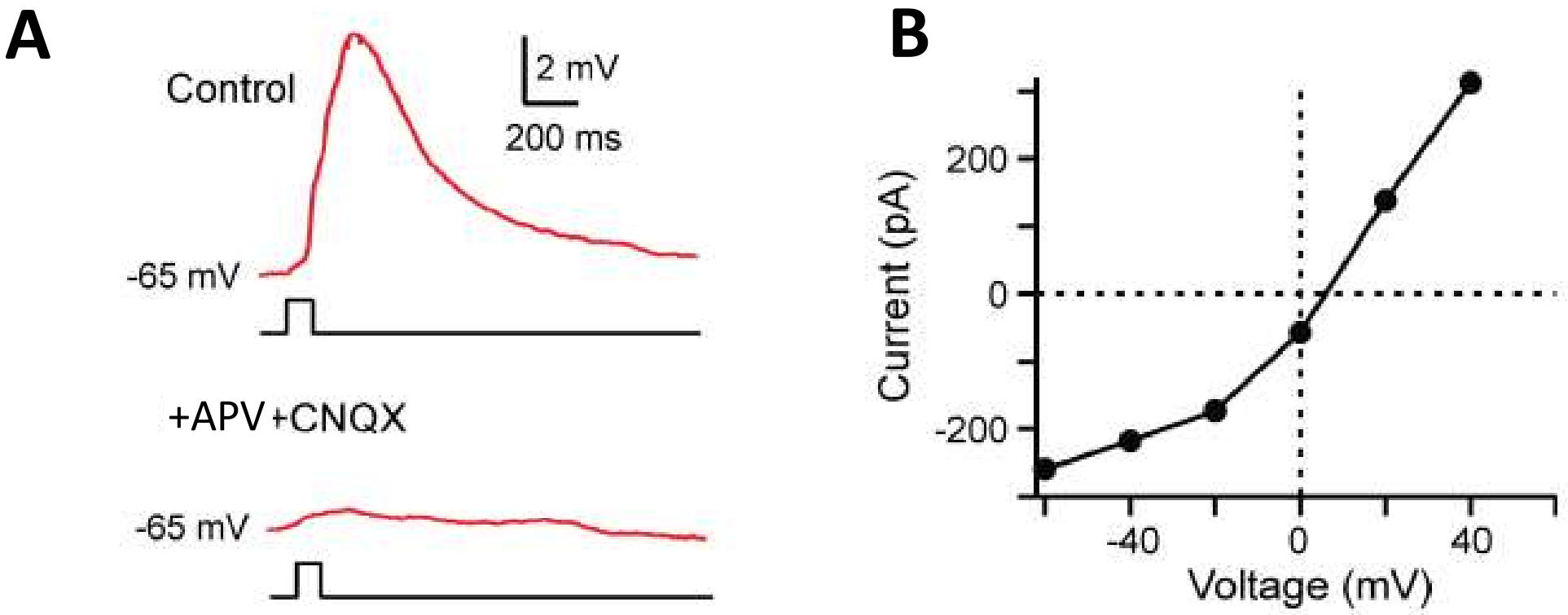

(A) Uncaging RuBi-Glutamate evokes an aEPSP on a mouse cortical layer 2/3 pyramidal neurone. Adding APV (40 μM) and CNQX (20 μM) blocked the uncaging response. (B) Representative *I-V* plot of an uncaged Rubi-Glutamate response. Note the reversal at +10 mV, indicating that the responses are mediated by glutamate receptors.

Fino et al., (2009). Front Neural Circuits 3:2. DOI: 10.3389/neuro.04.002.2009.

RuBi-GABA

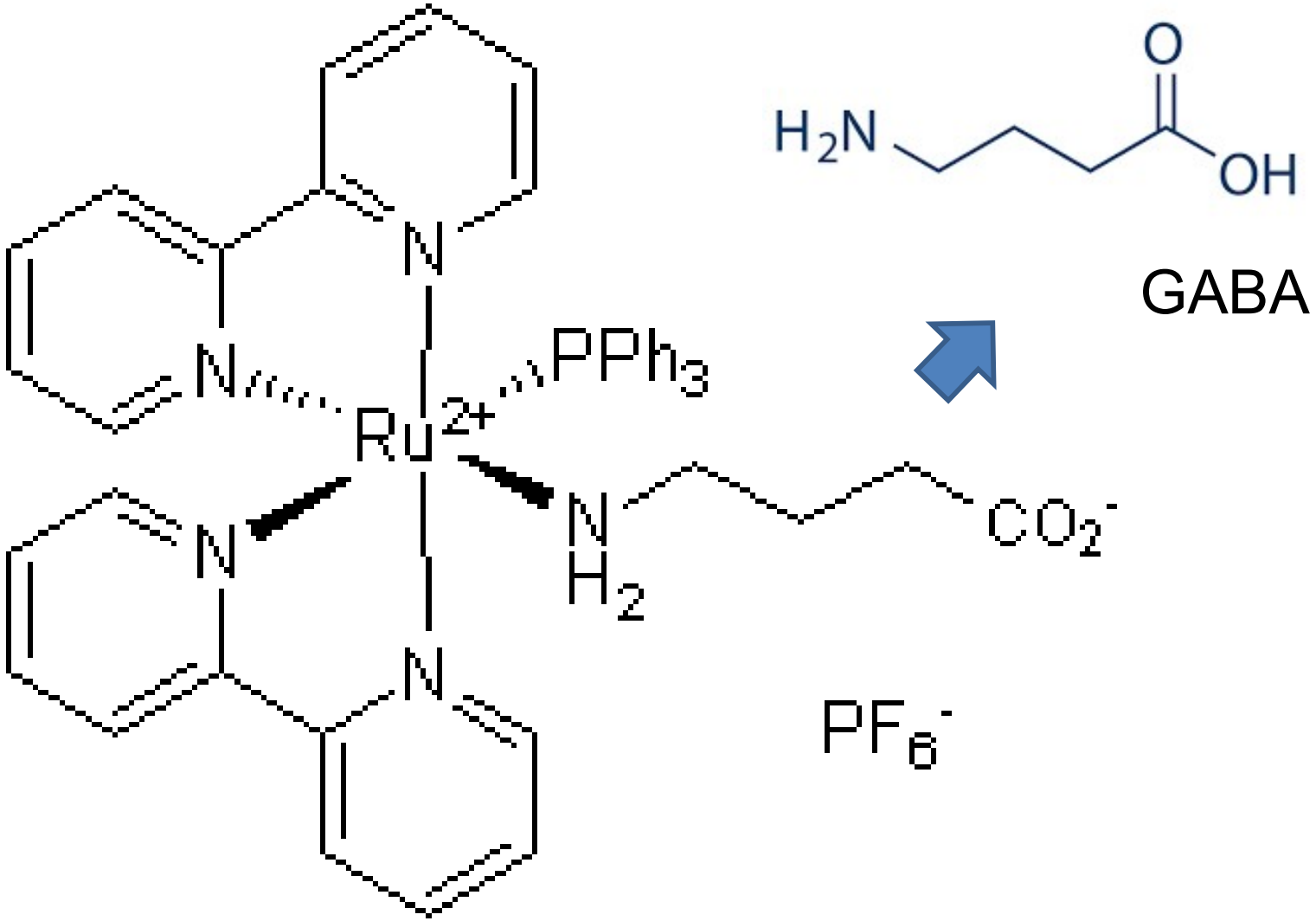

Ruthenium bipyridine-triphenylphosphine caged-GABA

RuBi-GABA

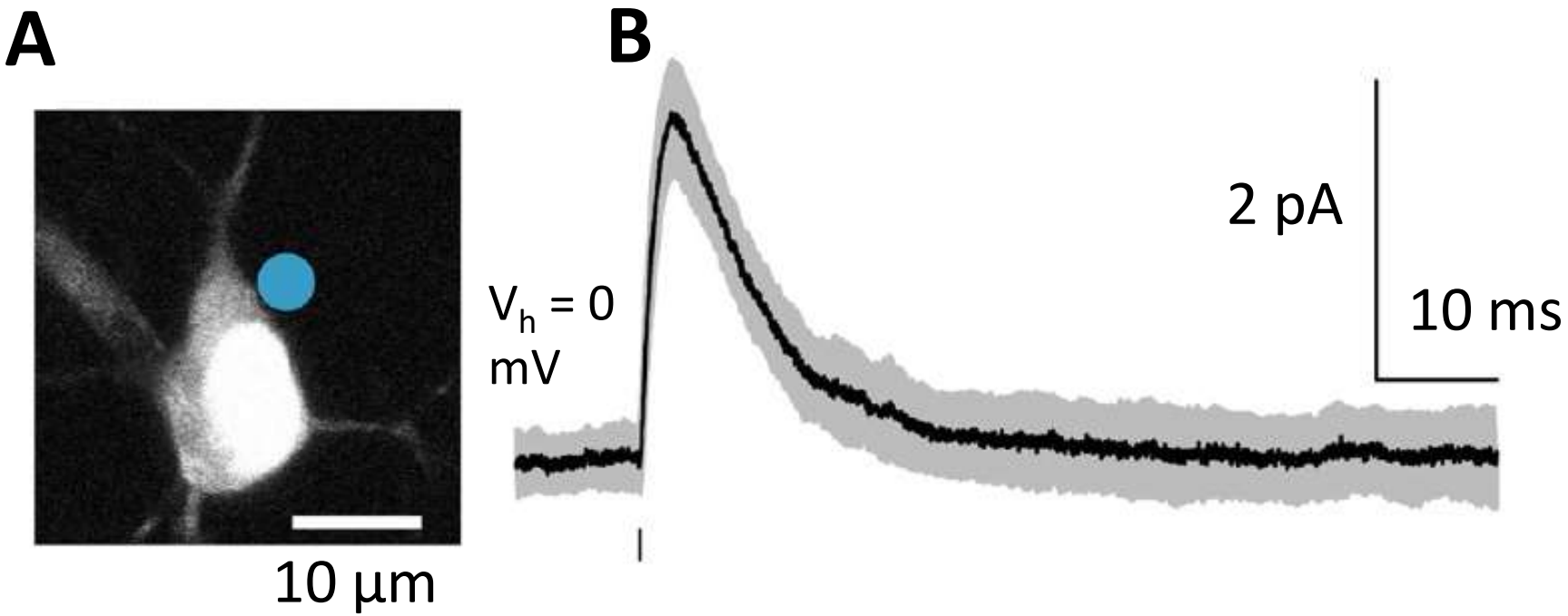

GABA photorelease from RuBi-GABA. (A) Mouse cortical layer 2/3 pyramidal neurone loaded with **Alexa Fluor 594**. RuBi-GABA (5 µM) was applied in the bath. Cyan dot indicates site of uncaging with **473 nm laser light (blue)**. (B) Average GABA outward current (black) and SD (grey) of 50 successive uncaging responses. The black bar below the trace indicates the uncaging laser pulse (0.5 ms; 30 mW).

Rial Verde et al., (2008). Frontiers in Neural Circuits 2:2
DOI:10.3389/neuro.04.002.2008

RuBi-GABA

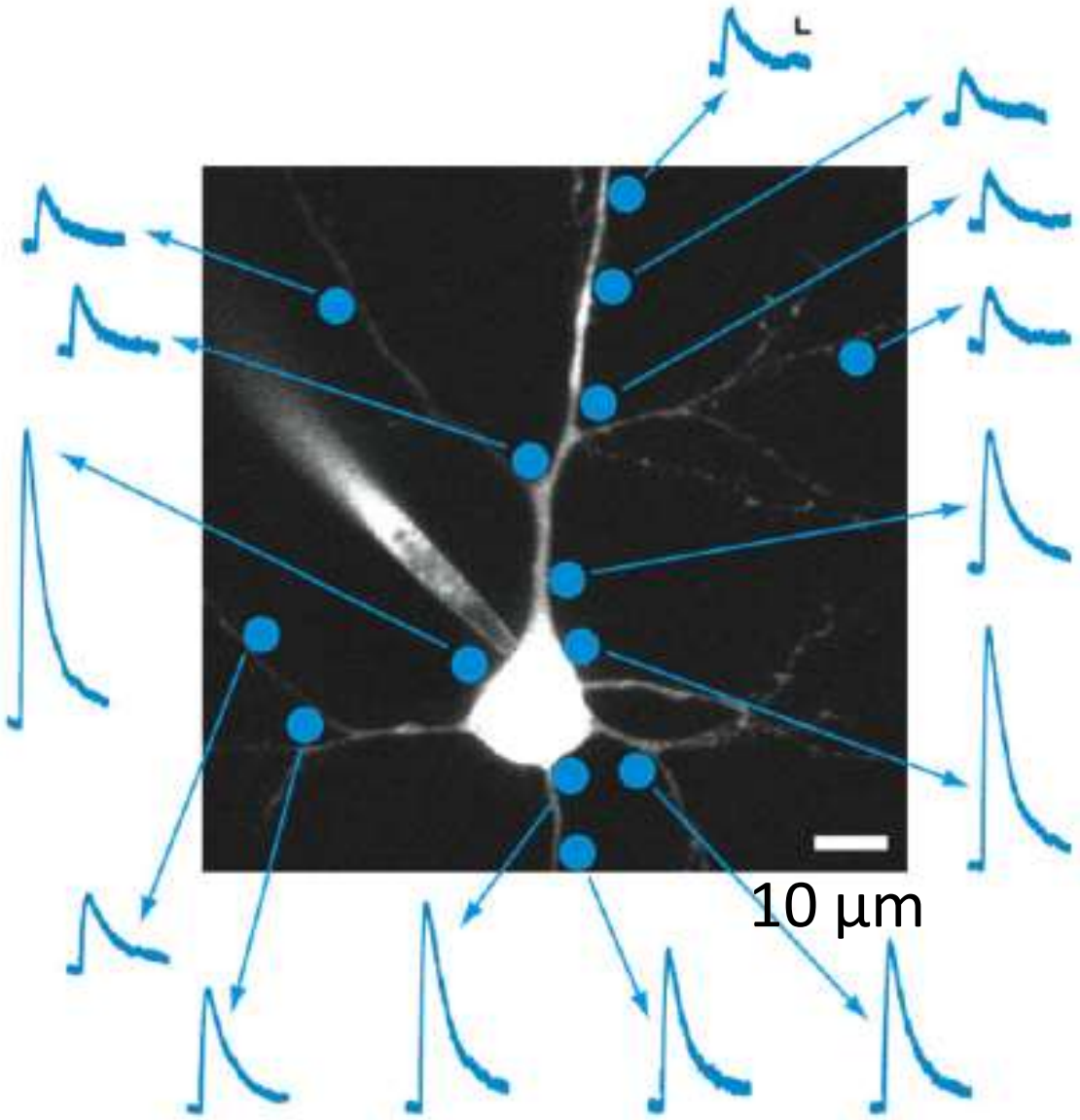

Mapping GABAergic responses in an individual neurone by uncaging RuBi-GABA (5 µM), using 0.5 ms 473 nm laser pulses of the same intensity at different positions along the cell body, dendrites, and axon of a mouse layer 2/3 pyramidal neurone. Scale bar: 5pA, 50 ms. V_h=0 mV

Rial Verde et al., (2008). Frontiers in Neural Circuits 2:2
DOI:10.3389/neuro.04.002.2008

RuBi-GABA

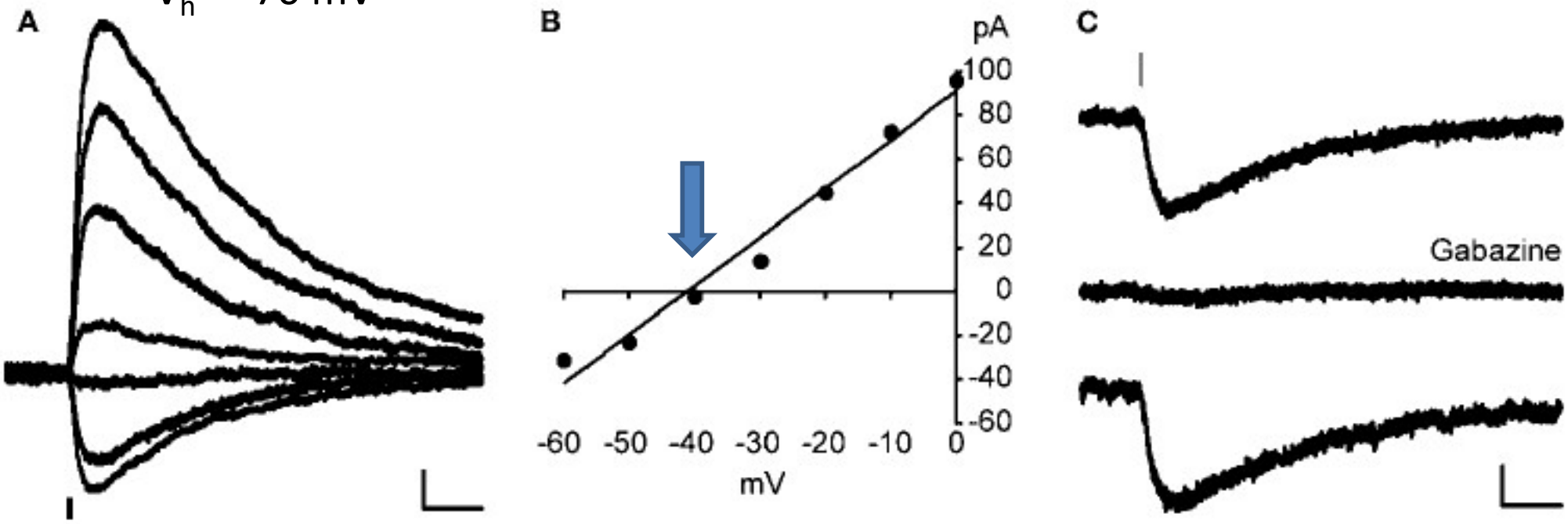

(A) RuBi-GABA uncaging currents recorded at different holding potentials (+10 mV steps; from -70 to 0 mV) showing the uncaging-induced current reversal close to E_{cl} (−43 mV). Black bar below the traces indicates the uncaging laser pulse. (B) *I-V* plot of the peak amplitudes shown in (A). (C) Average RuBi-GABA uncaging response before (top), during 20 μM gabazine application (centre), and after drug wash out (bottom), indicating that the response is mediated by GABA receptors. Scale bars:10 pA, 50 ms.

Rial Verde et al., (2008). Frontiers in Neural Circuits 2:2
DOI:10.3389/neuro.04.002.2008

Quantum dots

- **Quantum dots (QDs),** are nanometre-sized man-made colloidal semiconductor crystals (artificial atoms) with specific fluorescence properties, that have many commercial applications including LEDs, TVs, smart phones, solar cells, diode lasers, transistors as well as bioimaging.

- They are composed of a heavy metal core, such as cadmium, selenium or cadmium telluride with an intermediate unreactive zinc sulfide shell and a customized outer coating of different bioactive molecules tailored to a specific application such as antibodies, peptides *etc*.

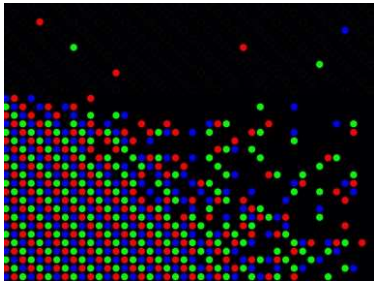

Quantum dots

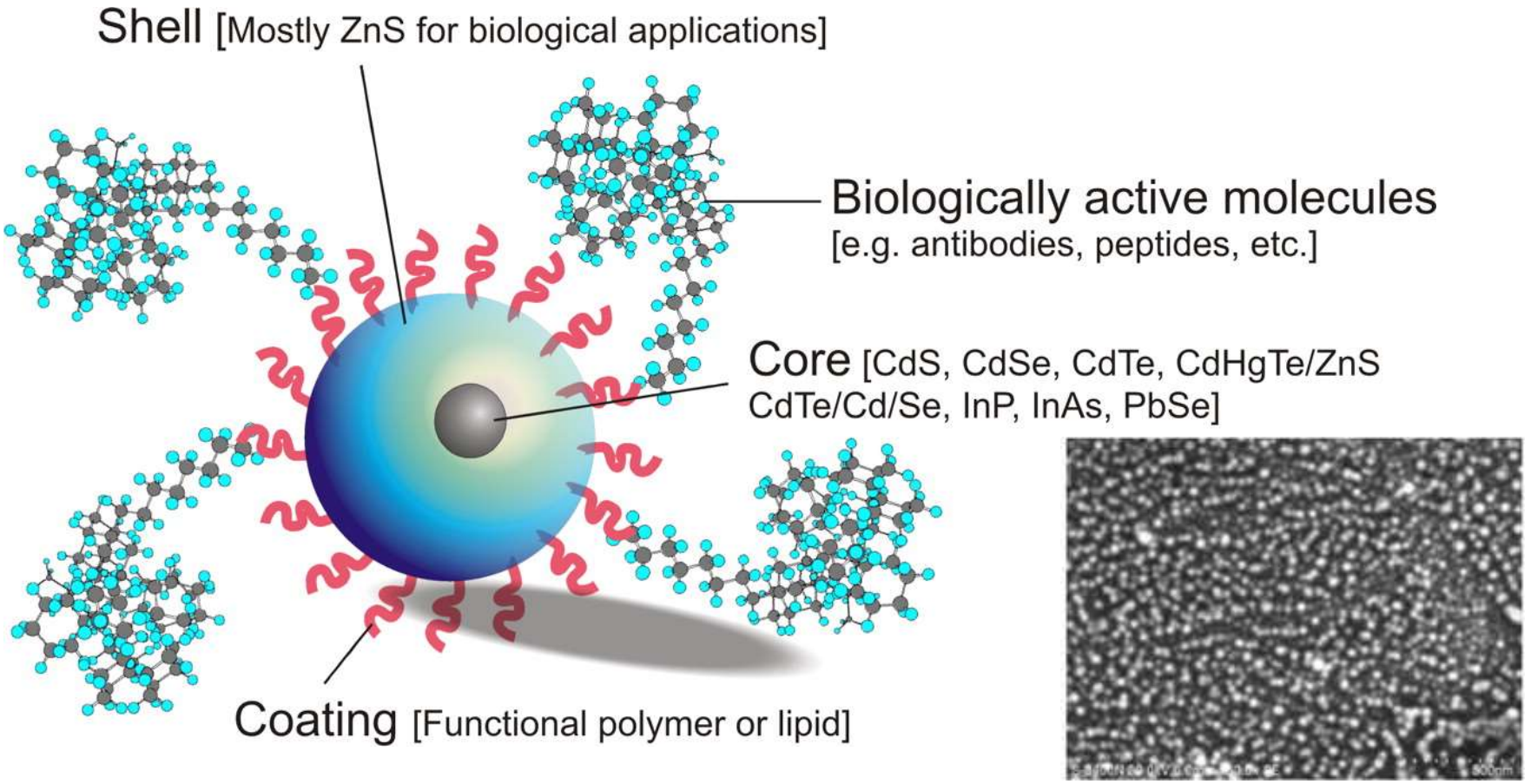

Structure of a semiconductor fluorescent quantum dot nanocrystal. The heavy metal core is responsible for the fluorescence properties of the quantum dot. The non-emissive shell stabilizes the core, whereas the coating layer provides anchor sites to organic and biological ligands such as antibodies, peptides, and other organic molecules.

Quantum dots

- Their small size (2-10 nm; 10-50 atoms) enables their optical and electronic properties to be different from those of bulk materials ("quantal" behaviour). QDs emit light of specific wavelengths if excited by light or electricity, determined by their size and shape, thus it is possible to control their emission wavelengths by tuning their size. Smaller QDs emit shorter wavelengths: violet, blue or green light, while bigger QDs emit longer wavelengths: yellow, orange or red light.

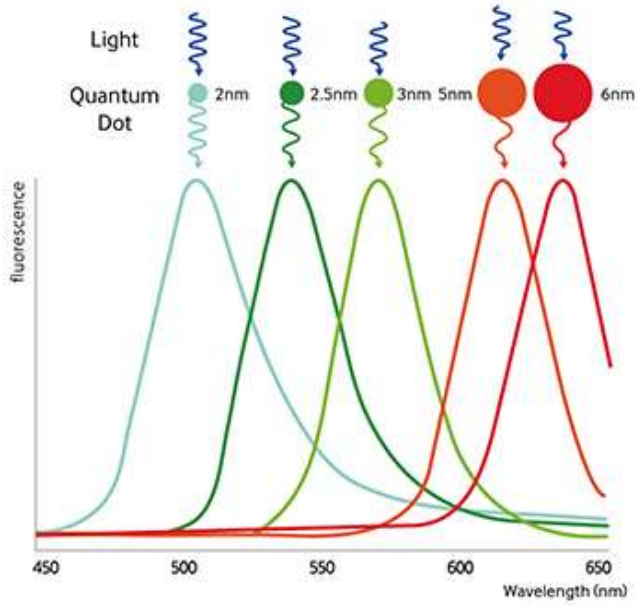

Gaussian emission spectra as a function of size for the same quantum dot material. The coloured spheres represent the size decrease of the particle

Quantum dots

Photoluminescence of alloyed CdSxSe1-x/ZnS quantum dots of 6 nm diameter. The material emits different colour of light by tuning the composition.

Quantum dots

- In neuroscience, they allow experimenters the unique ability to directly visualise and track individual biomolecular processes *e.g.* membrane neurotransmitter receptor movements, using a fluorescence microscope.

- Various fluorescent reporter dyes have been traditionally used in bioimaging but suffer from low quantum yield and poor photostability. QDs are considered superior in being brighter and more stable. QDs are water-dispersible, thus can be used for *in vitro* and *in vivo* imaging. QDs should not be toxic or interfere with cellular function.

- The 2023 Nobel Prize in chemistry was awarded to Moungi Bawendi, Louis Brus and Alexei Ekimov for the discovery and synthesis of quantum dots.

Quantum dots

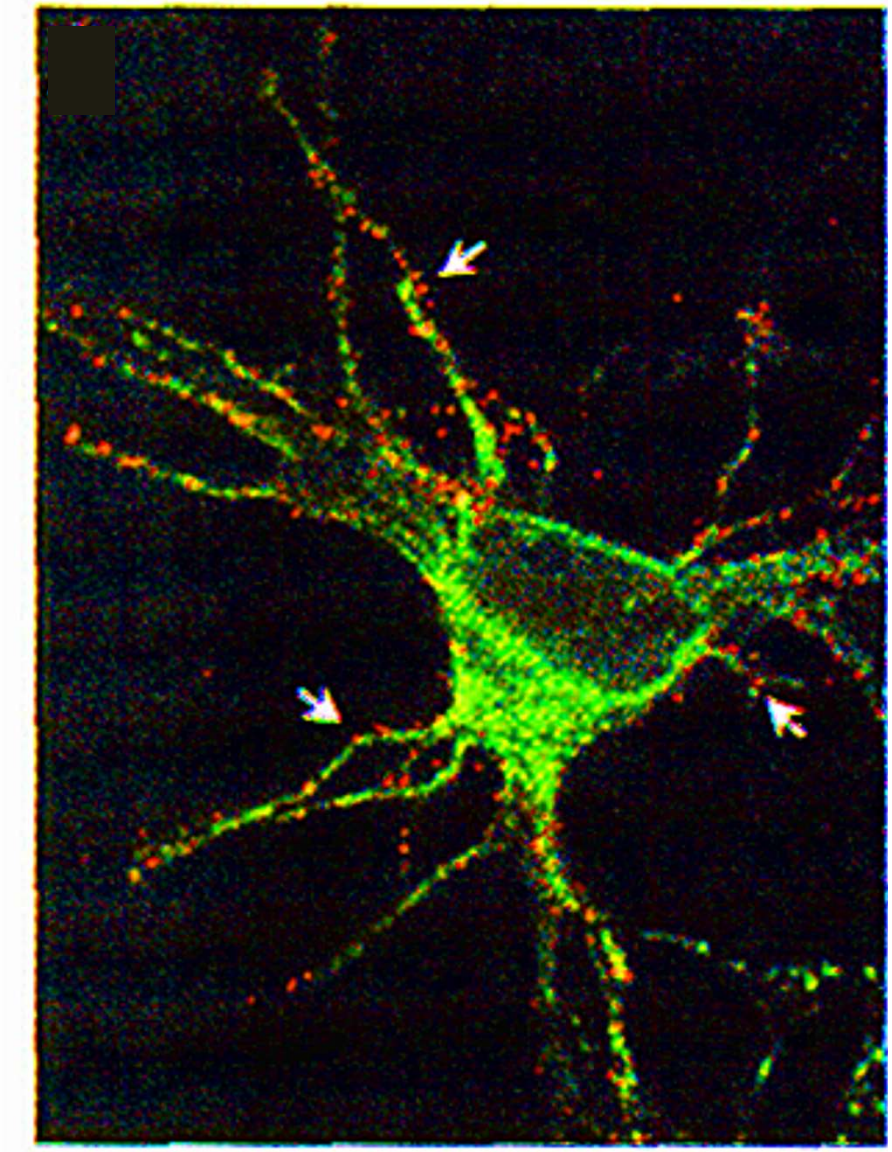

QDs as a marker for GlyR localization (red dots) in cultured spinal cord neurones. QD-GLyRs are detected over the somatodentritic compartment identified by microtubule-associated protein-2 (MAP-2) immunofluorescence (neuronal cytoskeletal marker: green). Arrows mark clusters of QD-GlyRs located on dendrites.

Dahan et al., (2003). Diffusion dynamics of glycine receptors revealed by single–quantum dot tracking. Science *302,* 442-445.

Quantum dots

Fluorescence image of a 625 QD-coated pipette (left) and an uncoated pipette ejecting Alexa Fluor 488 (right).

Another useful application for QDs is in the targeting of visually-identified neurones for patch-clamp recording which is usually hampered by poor visualization of pipette tips in deep brain tissue. When quantum dots are coated onto patch pipettes, it is possible, using strong two-photon contrast, to observe pipette and neurone at deeper penetration depths than with current two-photon imaging of fluorophores (*e.g.* Alexa Fluor dyes) that are continuously expelled from the pipette during the approach, thereby creating a "shadow" around a labelled or unlabelled neurone. **Andrásfalvy et al., (2014). Nat Methods. (12):1237-1241.**

Quantum dots

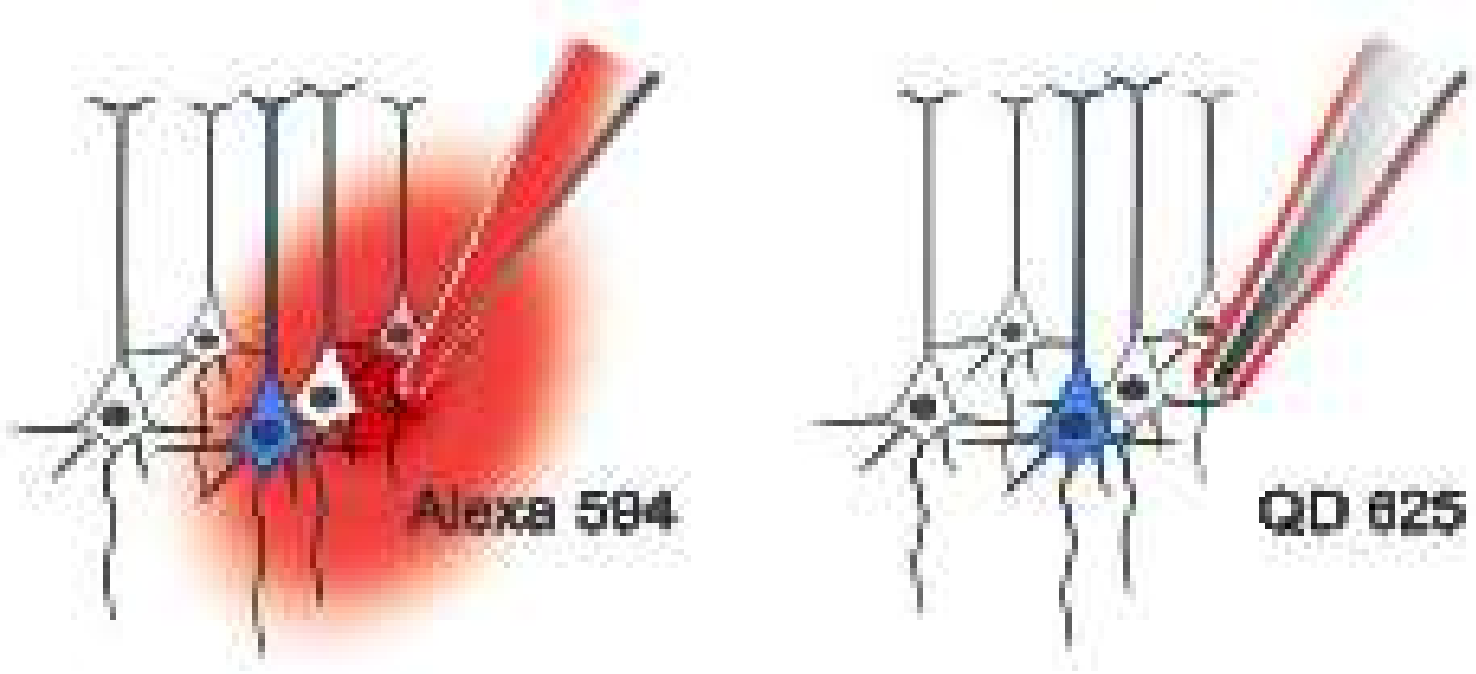

Schematics of the classic approach for pipette visualization during shadow patching (left) and the new approach (right) using QD-coated pipettes(red).

Andrásfalvy et al., (2014). Nat Methods. (12):1237-1241.

Quantum dots

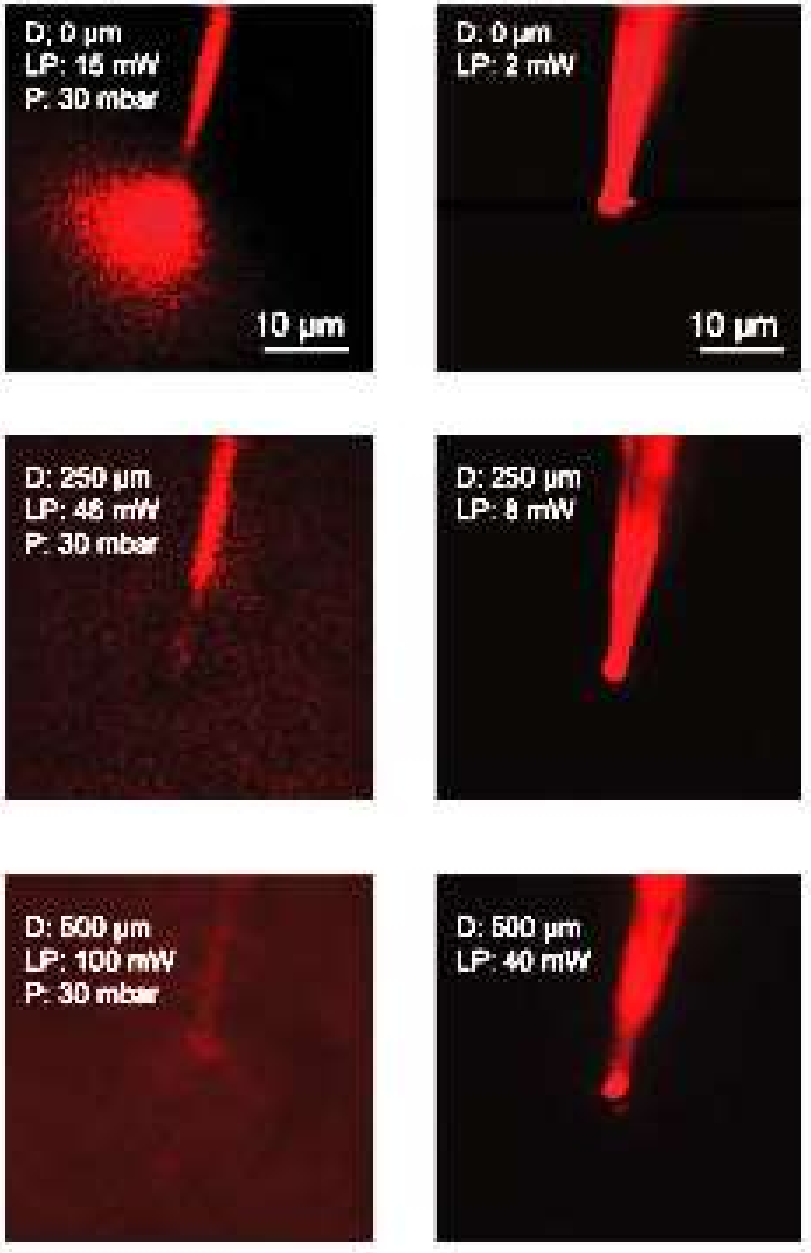

Alexa Fluor 594-filled pipettes (left) or **625 QD**-coated pipettes (right) were imaged at different depths (D) in the mouse brain at the indicated ejection pressure (P) and laser power (LP). Images are the average of 10 frames, except for Alexa Fluor at 500 µm (100 frames average).

Andrásfalvy et al., (2014). Nat Methods. (12):1237-1241.


"That's all Folks!"


buon Natale
©bs09